Image Compression using ITT and ICT and a Novel Variable Quantization Technique

Soni Prattipati

A Thesis

in

The Department

of

Electrical and Computer Engineering

Presented in Partial Fulfillment of the Requirements

for the Degree of Master of Applied Science (Electrical and Computer Engineering)
at

Concordia University

Montreal, Quebec, Canada

January 2014

CONCORDIA UNIVERSITY
SCHOOL OF GRADUATE STUDIES

This is to certify that the thesis prepared

By: Soni Prattipati

Entitled: Image Compression using ITT and ICT and a Novel Variable Quantization Technique

and submitted in partial fulfillment of the requirements for the degree of

Master of Applied Science

Complies with the regulations of this University and meets the accepted standards with respect to originality and quality.

Signed by the final examining committee:

_____ Chair
Dr. S. Hashtrudi Zad

_____ Examiner, External
Dr. Rama Bhat (MIE) To the Program

_____ Examiner
Dr. M. Omair Ahmad

_____ Supervisor
Dr. M.N.S. Swamy

Approved by: _____
Dr. W. E. Lynch, Chair
Department of Electrical and Computer Engineering

_____20_____ _____
Dr. Christopher W. Trueman
Interim Dean, Faculty of Engineering and Computer Science

ABSTRACT

Image Compression using ITT and ICT and
a Novel Variable Quantization Technique

Soni Prattipati

The need for novel transform coding techniques promising improved reconstruction and reduced computational complexity in the field of image and data compression is undeniable. Currently, there is a prevalent use of the integer adaptation of the popular discrete cosine transform (DCT) with fixed quantization in the video compression domain due to its ease of computation and adequate performance. However, there cannot be a single method or technique that would not only provide maximum compression possible, but also offer the best quality for different types of images. The influence of specific features of the image, such as its structure and content, on the quality of reconstructed image after decompression cannot be ignored. This thesis intends to utilize this aspect and identify areas where an alternative to integer DCT (ICT) for image compression can be proposed. There exist polynomial-based orthogonal transforms like discrete Tchebichef transform (DTT), which possess valuable properties like energy compaction, but are potentially unexploited in comparison with DCT. This thesis examines, in detail, where DTT stands as a viable alternative to DCT for lossy image compression based on various image quality parameters. It introduces a multiplier-free fast implementation of integer DTT (ITT) of size 8×8 that significantly reduces the computational complexity.

Normally, images have detail spread across them in a non-homogenous manner. Hence, when the image is divided into blocks, some blocks might have intricate detail, whereas the amount of detail in some might be very sparse. This feature is exploited in this thesis by proposing a technique to adapt the quantization performed during compression according to the characteristics

of the image block. The novelty of this variable quantization is that it is simple to implement without much computational or transmission overhead. The image compression performance of ITT and ICT, using both variable and fixed quantization, are evaluated and compared for a variety of images. Eventually, the cases suitable for ITT-based image compression employing variable quantization are identified.

Acknowledgements

I would like to express my heartfelt gratitude to my research supervisor, Dr. M.N.S Swamy for his guidance and support during the course of my work. I can never thank him enough for the patience and empathy he showed me through out. His knowledge and expertise have been critical in getting my work completed. It has been a great learning experience and I am truly happy for having got this opportunity to work under his direction. He has been a huge source of inspiration and a leader in the true sense.

I would like to extend my gratitude to Dr. Meher for his help and valuable insights during the research.

I bow to my teachers for the education imparted to me.

I thank my family for all the love and affection bestowed on me. They believed in me and encouraged me even at times when I doubted myself...

I would also like to thank my friends who stood beside me and have made this voyage fun and enjoyable, so far.

Table of Contents

List of Figures

List of Tables

List of Acronyms and symbols

AD	*average difference*
bpp	*bits per pixel*
CR	*compression ratio*
DCT	*discrete cosine transform*
DFT	*discrete Fourier transform*
DTP	*discrete Tchebichef polynomial*
DTT	*discrete Tchebichef transform*
HEVC	*high efficiency video coding*
HVS	*human visual system*
ICT	*integer discrete cosine transform*
ITT	*integer discrete Tchebichef transform*
JPEG	*joint photographic expert group*
LMSE	*Laplacian mean squared error*
MD	*maximum difference*
NAE	*normalized absolute error*
NK	*normalized cross-correlation*
nzp	*non-zero element position in the matrix*
PQE	*picture quality evaluation*
PSNR	*peak signal to noise ratio*
RLE	*run length encoding*
RMSE	*root mean square error*

SAM	*spectral activity measure*
SC	*structural content*
SFM	*spatial frequency measure*
$\alpha(n)$	step function with unit jumps
Δ	forward difference operator
$t_k(n)$	k^{th} Tchebichef polynomial
$t_m(n)$	m^{th} Tchebichef polynomial
$\tau\ (k,n)$	DTP transfer function
$d(k,N)$	squared norm of the DTP
τ	DTT transform kernel
$\hat{\tau}$	ITT transform kernel
$\odot$	element-by-element multiplication
$\hat{Q}$	factorization matrix for ITT
$F(i,j)$	$(i,j)^{th}$ DFT coefficient of the original image
M	number of pixels in the image in horizontal direction
N	number of pixels in the image in vertical direction
R_f	row Frequency
C_f	column Frequency
$x_{i,j}$	$(i,j)^{th}$ pixel value of the original image
$x'_{i.j}$	$(i,j)^{th}$ pixel value of the reconstructed image

Chapter 1

Introduction

1.1 Background

From times immemorial, pictures have been widely employed by mankind not just for entertainment but also to communicate and document important events. The story of pictures and their evolution from the initial scratches that a cave man might have made on the walls of his cave to the current day format is fascinating. There have been some crucial advancements such as invention of the printing press, photograph machine and video camera which revolutionized the field of imaging. Despite the evolution of advanced languages along with their respective scripts in the course of time, modern day communication still relies heavily on images to convey information. The age old adage 'A picture is worth a thousand words' could not have been more correct. An image transcends the language barriers and other limitations that a written message might have. It provides the viewer the freedom of framing one's own opinions based on one's interpretation of the image.

The invention of electronic storage devices has altered the world of data storage forever. Initially, data was stored in analog format but it soon paved the way for digitization which offered numerous advantages like noise immunity, bandwidth conservation and ease of encoding [1]. With the advent of computers and the ensuing digital revolution, images started being stored in digital format. In this format, the image is envisioned to be a collection of multiple small dots

called pixels. The more the number of pixels in an image, the higher is the resolution of the image [2]. Each pixel is assigned an intensity value which is stored in binary format. In case of color images, each pixel carries color information too in addition to the intensity. With an increasing demand for high quality images and invention of high resolution cameras, the number of pixels needed to represent an image has increased. As a result, the size of data representing the image has increased tremendously. Though this might seem to be an almost bearable burden in case of storing an image, it has proved to be quite an onerous task if the same image is to be transmitted. Transmitting and receiving a single image would take ridiculously long time and the channel bandwidth would be clogged. This situation demanded for a solution, where the image can be represented by a reduced volume of data while still maintaining its quality. This paved the way for image compression [3].

Image compression mainly exploits the presence of inherent redundancy and irrelevant details in images to reduce the size of the data needed to represent the image. The various compression techniques available can be broadly classified as lossy and lossless procedures based on the type of details that are eliminated to reduce the amount of data. Lossless compression techniques avoid redundancy in the data and promise an exact reproduction of the image from the compressed data by avoiding just the redundant information. However, the resultant amount of compression achieved with this procedure may not be high. Lossy compression techniques on the other hand strip off some of the insignificant details of the image in addition to the redundant information to achieve high levels of compression. As a result, the decompressed image might not be an exact replica of the original. These reasons make lossless compression techniques more suitable for applications, where image quality gains precedence over the size of the image. Lossy compression is preferred for applications where a minor loss of quality is acceptable provided the

image data size is decreased. Over a period of time with the dawn of communication and internet revolutions and development of improved compression algorithms, lossy compression techniques have become more popular over lossless techniques. For instance, wide use of image sharing and video streaming necessitated the need to transmit huge volumes of data in real time without any bandwidth congestion. This is possible only with lossy image compression. Applications like space research and defense often require huge volumes of video data to be transmitted, analyzed and a suitable response triggered instantaneously. This mandates the use of compression techniques to accelerate the transmission procedure, which consumes the major portion of the total response time.

In transform-coded compression techniques, the image undergoes transformation before being encoded. This removes the redundancy in the data being transmitted thereby resulting in compression. If the transformed image data is subjected to quantization before encoding, some of the insignificant data in the image is avoided along with the redundant details leading to greater compression. However a balance needs to be maintained such that the loss of data does not translate into image quality deterioration beyond a tolerable level. There are many transforms currently in use to compress an image, each having its own pros and cons, thus making certain transforms ideal for compression of certain class of images.

1.2 Scope of the Thesis

The discrete Tchebichef transform (DTT), based on a polynomial kernel derived from discrete Tchebichef polynomials (DTPs), was introduced in [4] and was developed later into an orthogonal transform in [5]. The discrete cosine transform (DCT), which originates from the trigonometric representation of the Tchebichef polynomials of the first kind, has its image

compression potential exhaustively investigated. Numerous fast DCT algorithms [6]–[8] have been developed and multiple DCT-based compression techniques have been established. DTT exhibits energy compaction and de-correlation properties that are very much comparable with those of DCT. For a block size 8×8 and correlation coefficient 0.9, the de-correlation efficiencies of DTT and DCT are 97.34% and 97.82%, respectively [9], [10]. The first five diagonal elements of the transformation matrix result in energy packing efficiencies of 97.41% and 97.6% for DTT and DCT, respectively [9], [10]. DTT can be shown to conform easily to an integer representation without the need for approximation unlike the Integer counterpart of DCT. This reveals that DTT could be a potential competitor to DCT for certain classes of images.

As DTT is not as extensively explored as DCT, there is scope for research to identify areas where DTT could offer a better performance. DCT's integer counterpart, integer cosine transform (ICT), is being widely used for video compression due to ease of computation [11]. A given compression technique does not yield similar response to different genres of images and in some specific situations DCT-based compression might not be the perfect choice available. Hence, it is definitely worth the effort to evaluate the performance of integer DTT (ITT) with respect to that of ICT proposed in [11] for compression of some special images. This work aims at identifying areas where ITT stands up to be a viable alternative to ICT for lossy image compression based on various image quality assessment parameters. Based on these findings, it would be possible to predict if an image is suited for ITT-based compression or ICT-based compression. An ITT for a block size of 8×8 is introduced here, whose computational complexity is compared with that of ICT. The proposed fast implementation is intended to be completely multiplier-free and should be comparable with other popular fast integer multiplier-free DCT implementations.

This work also intends to further enhance the lossy compression algorithm by including a variable quantization technique thereby ensuring better image quality even at higher compression rates. Quantization is a significant step during the lossy image compression procedure and optimizing it for better performance without an increase in computational complexity is highly desirable. It is unusual for an image to have a homogenous distribution of data all over. As a result selecting a distinct quantization matrix optimized for each individual image block is appealing, but it would require transmitting the quantization information along with each block of the image. This significant transmission overhead defeats the very purpose of compression. Hence, this thesis evaluates the performance of ITT with respect to that of ICT proposed in [11] for compression of some special images using an improved variable quantization technique. This method intends to eliminate the need to maintain any predefined set of matrices at both ends. This method also plans to ensure that there would be no need for extra bits in order to transmit the variable quantization information with a special encoding technique, thus making the proposed quantization process free of any additional transmission overhead.

1.3 Organization of the thesis

The rest of the thesis is organized as follows. Chapter 2 deals with introduction to discrete polynomials, DTP in particular, its history, definition and properties. Derivations for the DTT, its inverse and its significance in image compression are explained. An Integer DTT for a block size of 8×8 is deduced whose realization is comparable with that of the ICT.

Chapter 3 includes a description of the image compression procedure more in detail and elucidates the various steps involved. It proposes a fast implementation of the DTT which is completely multiplier-free and its computational complexity is compared with other popular fast

integer multiplier-free DCT implementations. It gives the role played by a transform in the compression process and emphasizes the importance of choosing a suitable transform to achieve desired compression. It also explains the various image assessment parameters employed to measure the quality and level of compression of the image. Experimental results comparing these parameters for various images using ITT and ICT compression techniques are presented and analyzed.

Chapter 4 presents the necessity for variable quantization during compression. It compares the pros and cons of using an adaptive quantization technique over the conventional quantization procedure. It introduces a novel way of incorporating the variable quantization into the compression process without any significant increase in the computational or transmission overhead. Experimental results of compression performance for images using variable and conventional quantization for both the ITT-and ICT-based compression techniques are exhibited and discussed.

Chapter 5 summarizes the work done and consolidates the findings along with their significance in current world. Probable areas for further research are also identified and discussed.

Chapter 2

Integer Tchebichef Transform

Any signal conveying information can be represented as a function of one or more independent variables. For instance, the information in an image can be represented by a brightness function of spatial variables. The independent variables used for representation could be continuous or discrete depending on the signal being continuous or discrete. It is possible to represent a continuous signal using discrete variables and obtain transformations which could not have been normally realized. So, discrete time representation of signals is preferred over continuous time representation for its flexibility. Discrete signal processing deals with discrete signals namely, their representation, transformation and manipulation.

Transforms refer to conversion of signals between different domains like time and frequency. The representation of a signal in multiple domains makes it suitable for various applications like compression, analysis, detection, filtering etc. There are different popular discrete transforms like discrete Cosine, discrete Fourier, discrete Wavelet, discrete Hartley transforms. Each of these transforms represents the signal in varied domains, bringing out specific innate characteristics which are suitable for different applications.

Discrete signals can be denoted using linear combination of sinusoidal or complex exponential sequences. Thus polynomials which are orthogonal in particular, are widely employed to represent the signals in view of their efficient data fitting and approximation abilities [12]. Some

of the popular discrete orthogonal polynomials are Hahn, Meixner, Krawtchouk and Charlier [13].

2.1 Discrete Tchebichef Polynomial

Discrete Tchebichef polynomials (DTP) [9], [10], [14], [15] are the class of hyper geometric orthogonal polynomials associated with the distribution dα(n) of Stieltjes type, where α(n) is a step function with unit jumps at support points n = 0, 1, …,N−1 [16]. They are a special case of Hahn polynomials, which are classic discrete orthogonal polynomials and discrete analog of popular Jacobi polynomials [17].

If Δ is the forward difference operator, the DTP is defined by the difference formula

$$t_k(n)=k!\,\Delta^k\left[\binom{n}{k}\binom{n-N}{k}\right] \text{ for } k = 0,1,\ldots N-1 \quad (2.1)$$

where $t_k(n)$ is the k^{th} Tchebichef polynomial.

DTP exhibits important properties like orthogonality, recurrence and normalization which can be used to define a related transfer function τ(k,n) where k, n correspond to the indices of the frequency and time components, respectively, as shown in [9], [10], [14].

2.1.1 Properties of DTP

A. ***Orthogonality:*** DTPs are orthogonal with respect to a unit weight function

$$\sum_{n=0}^{N-1} t_k(n)t_m(n) = \delta_{km}\, d(k,N) \qquad (2.2)$$

where $t_k(n)$ and $t_m(n)$ are the k^{th} and m^{th} Tchebichef polynomials, respectively, and $d(k,N)$ is the squared norm of the DTP defined as

$$d(k,N) = \sum_{n=0}^{N-1} [\, t_k(n)]^2 \qquad (2.3)$$

The squared norm of the DTP can also be written as

$$d(k,N) = \frac{N\,(N^2-1)(N^2-2^2)\ldots(N^2-k^2)}{2k+1} \qquad (2.4)$$

B. ***Direct Representation:*** DTP can be evaluated using the closed form expression

$$t_k(n) = k! \sum_{i=0}^{k} (-1)^{k-i} \binom{N-1-i}{k-i} \binom{k+i}{k} \binom{n}{i} \qquad (2.5)$$

C. ***Recurrence Relation:*** DTPs satisfy a three-term recurrence relation given by

$$t_k(n) = \left[\left(\frac{2k-1}{k}\right) t_1(n)\right] t_{k-1}(n) - \left[\left(\frac{k-1}{k}\right) (N^2-(k-1)^2\right] t_{k-2}(n) \qquad (2.6)$$

for k $\geq$2 with $t_0(n) = 1$, $t_1(n) = 2n-N+1$. This formula is useful for a fast evaluation of polynomials of higher degrees.

D. ***Symmetry:*** The DTP satisfies the symmetry property

$$t_k(N-1-n) = (-1)^k t_k(n) \qquad (2.7)$$

E. ***Normalization of the DTP:*** The system defined in (2.1) is orthogonal. Every orthogonal system can be normalized by replacing $t_m(x)$ by $\langle t_m . t_m \rangle^{-\frac{1}{2}} t_m(x)$ [15], where $\langle . \rangle$ is the scalar product. In view of (2.3), orthonormal DTP, denoted by $\tau_k(n)$, is given by

$$\tau_k(\mathrm{n}) = \frac{t_k(n)}{\sqrt{d(k,N)}} \qquad (2.8)$$

As a consequence, the recurrence relation in (2.6) may be rewritten for orthonormal DTPs in the form [5]

$$\tau_k(\mathrm{n}) = (a_{\,1}n + \ a_{\,2})\tau_{k-1}(\mathrm{n}) + \ a_{\,3}\tau_{k-2}(\mathrm{n}) \qquad (2.9)$$

With $\tau_0(\mathrm{n}) = \frac{1}{\sqrt{N}}$, $\tau_1(\mathrm{n}) = (2n + 1 - N)\sqrt{\frac{3}{N(N^2-1)}}$ where

$$a_1 = \frac{2}{3}\sqrt{\frac{4k^2-1}{N^2-k^2}}\ , a_2 = \frac{1-N}{k}\sqrt{\frac{4k^2-1}{N^2-k^2}}\ , a_3 = \frac{1-k}{k}\ .\ \frac{2k+1}{2k-3}\sqrt{\frac{N^2-(k-1)^2}{N^2-k^2}}$$

From the Discrete Tchebichef Polynomial and its various properties a Discrete Tchebichef Transform (DTT) is derived.

2.2 Discrete Tchebichef Transform

In the DTT domain, the transformed sequence, $Y(k)$, of an input data sequence, $x(n)$, is given by

$$\mathrm{Y(k)}=\sum_{\mathrm{n=0}}^{\mathrm{N\text{-}1}} \tau(\mathrm{k,n})\mathrm{x(n)} \quad \text{for } k,n = 0,1,\ldots N\text{-}1 \qquad (2.10)$$

where $\tau(\mathrm{k,n})$ is the orthogonal basis of DTP denoted as $\tau_k(\mathrm{n})$ in (2.8) over an interval [0,N-1] and whose values can be got from the recurrence relation in (2.9). In the above equation k and n denote frequency and time indices, respectively.

The *inverse DTT* restores the input data when applied to the transform coefficients and is given by

$$x(n)=\sum_{k=0}^{N-1}\tau(k,n)Y(k) \qquad \text{for } k,n=0,1,..,N-1 \qquad (2.11)$$

For a 2-D input sequence $x(n_1,n_2)$, the *2-D DTT of order* $N\times M$ is defined as

$$Y(k_1,k_2)=\sum_{n_1=0}^{N-1}\sum_{n_2=0}^{M-1}\tau(k_1,n_1)\tau(k_2,n_2)x(n_1,n_2) \qquad (2.12)$$

for $k_1, n_1 = 0,1 \ldots, N-1$ and $k_2, n_2 = 0,1 \ldots, M-1$.

The *inverse 2-D DTT* is given by

$$x(n_1,n_2)=\sum_{k_1=0}^{N-1}\sum_{k_2=0}^{M-1}\tau(k_1,n_1)\tau(k_2,n_2)Y(k_1,k_2) \qquad (2.13)$$

for $k_1, n_1 = 0,1,\ldots, N-1$ and $k_2, n_2 = 0,1,\ldots, M-1$

All the properties of DTP discussed in Section 2.1.1 are applicable to DTT as well.

2.2.1 Integer Tchebichef Transform

Floating-point operations preserve full-precision value, but at the cost of increased resource consumption. Moreover, floating-point operations are not defined in all processors. Integer operations offer increased computational speed, decreased complexity, cost and power consumption. This sub-Section, discusses an integer Tchebichef transform of size 8×8 which greatly reduces the computational complexity.

Framework for Integer Transform Representation: The 2-D DTT of input data X, of size $N \times N$ given by (2.12), can also be expressed in the form below

$$Y = \tau X \tau' \qquad (2.14)$$

where τ is the '$N \times N$' transform and can be factorized as shown below to separate the integer and float numbers. Consider a variable

$$q(k) = \frac{p(k)}{\sqrt{d(k,N)}} \qquad (2.15)$$

where

$$p(k) = \begin{cases} k!k & \text{for } k=1 \\ k!(k+1) & \text{for } k=0,2,4,6 \\ k!(N-k) & \text{for } k=3,5,7 \end{cases}$$

and $d(k,N)$ is the squared norm of the DTP given by

$$d(k,N) = \frac{N(N^2-1)(N^2-2^2)\ldots(N^2-k^2)}{2k+1} \qquad (2.16)$$

Let $\boldsymbol{Q}$ be a '$N \times N$' diagonal matrix with $q(k)$ given in (2.15) as the diagonal element of the k^{th} row.

$$Q = \begin{pmatrix} q_0 & 0 & 0 & \ldots & 0 & 0 \\ 0 & q_1 & 0 & \ldots & 0 & 0 \\ 0 & 0 & q_2 & \ldots & 0 & 0 \\ \vdots & \vdots & \vdots & \ldots & \vdots & \vdots \\ 0 & 0 & 0 & \ldots & q_{N-2} & 0 \\ 0 & 0 & 0 & \ldots & 0 & q_{N-1} \end{pmatrix} \qquad (2.17)$$

For N = 8 the corresponding $\boldsymbol{Q}$ matrix would be

$$Q = \begin{pmatrix} 0.3536 & 0 & 0 & 0 & 0 & 0 & 0 & 0 \\ 0 & 0.0772 & 0 & 0 & 0 & 0 & 0 & 0 \\ 0 & 0 & 0.0772 & 0 & 0 & 0 & 0 & 0 \\ 0 & 0 & 0 & 0.0615 & 0 & 0 & 0 & 0 \\ 0 & 0 & 0 & 0 & 0.0403 & 0 & 0 & 0 \\ 0 & 0 & 0 & 0 & 0 & 0.0214 & 0 & 0 \\ 0 & 0 & 0 & 0 & 0 & 0 & 0.0615 & 0 \\ 0 & 0 & 0 & 0 & 0 & 0 & 0 & 0.0171 \end{pmatrix}$$

It is possible to express the transformation matrix τ as

$$\tau = \boldsymbol{Q}\hat{\tau} \qquad (2.18)$$

$$\hat{\tau} = \boldsymbol{Q^{-1}}\,\tau \qquad (2.19)$$

Hence evaluating (2.19) by substituting the values of τ from (2.9) and $\boldsymbol{Q}$ for $N = 8$ results in

$$\hat{\tau} = \begin{pmatrix} 1 & 1 & 1 & 1 & 1 & 1 & 1 & 1 \\ -7 & -5 & -3 & -1 & 1 & 3 & 5 & 7 \\ 7 & 1 & -3 & -5 & -5 & -3 & 1 & 7 \\ -7 & 5 & 7 & 3 & -3 & -7 & -5 & 7 \\ 7 & -13 & -3 & 9 & 9 & -3 & -13 & 7 \\ -7 & 23 & -17 & -15 & 15 & 17 & -23 & 7 \\ 1 & -5 & 9 & -5 & -5 & 9 & -5 & 1 \\ -1 & 7 & -21 & 35 & -35 & 21 & -7 & 1 \end{pmatrix} \qquad (2.20)$$

Consequently, from (2.18), the transform of (2.14) may be written as

$$Y=(\boldsymbol{Q}\hat{\tau})X\,(\boldsymbol{Q}\hat{\tau})' = \boldsymbol{Q}\,(\hat{\tau}\,X\,\hat{\tau}')\,\boldsymbol{Q} \qquad (2.21)$$

By utilizing the properties of a diagonal matrix the above equation can be expressed as

$$Y=(\hat{\tau}\,X\,\hat{\tau}')\odot\widehat{\boldsymbol{Q}} \qquad (2.22)$$

where ⊙ represents element-by-element multiplication and $\widehat{\boldsymbol{Q}}$.

$\hat{Q}$ can be obtained by multiplying the diagonal elements of

$$\widehat{\boldsymbol{Q}} = (diagonal\ elements\ of\ Q)_{NX1} \times (diagonal\ elements\ of\ Q)_{1XN} \quad (2.23)$$

For $N = 8$, $\widehat{\boldsymbol{Q}}$ is given by

$$\widehat{Q} = \begin{pmatrix} q_0^2 & q_0q_1 & q_0q_2 & q_0q_3 & q_0q_4 & q_0q_5 & q_0q_6 & q_0q_7 \\ q_0q_1 & q_1^2 & q_1q_2 & q_1q_3 & q_1q_4 & q_1q_5 & q_1q_6 & q_1q_7 \\ q_0q_2 & q_1q_2 & q_2^2 & q_2q_3 & q_2q_4 & q_2q_5 & q_2q_6 & q_2q_7 \\ q_0q_3 & q_1q_3 & q_2q_3 & q_3^2 & q_3q_4 & q_3q_5 & q_3q_6 & q_3q_7 \\ q_0q_4 & q_1q_4 & q_2q_4 & q_3q_4 & q_4^2 & q_4q_5 & q_4q_6 & q_4q_7 \\ q_0q_5 & q_1q_5 & q_2q_5 & q_3q_5 & q_4q_5 & q_5^2 & q_5q_6 & q_5q_7 \\ q_0q_6 & q_1q_6 & q_2q_6 & q_3q_6 & q_4q_6 & q_5q_6 & q_6^2 & q_6q_7 \\ q_0q_7 & q_1q_7 & q_2q_7 & q_3q_7 & q_4q_7 & q_5q_7 & q_6q_7 & q_7^2 \end{pmatrix} =$$

$$\begin{pmatrix} 0.1250 & 0.0273 & 0.0273 & 0.0218 & 0.0142 & 0.0076 & 0.0218 & 0.0060 \\ 0.0273 & 0.0060 & 0.0060 & 0.0047 & 0.0031 & 0.0017 & 0.0047 & 0.0013 \\ 0.0273 & 0.0060 & 0.0060 & 0.0047 & 0.0031 & 0.0017 & 0.0047 & 0.0013 \\ 0.0218 & 0.0047 & 0.0047 & 0.0038 & 0.0025 & 0.0013 & 0.0038 & 0.0011 \\ 0.0142 & 0.0031 & 0.0031 & 0.0025 & 0.0016 & 0.0009 & 0.0025 & 0.0007 \\ 0.0076 & 0.0017 & 0.0017 & 0.0013 & 0.0009 & 0.0005 & 0.0013 & 0.0004 \\ 0.0218 & 0.0047 & 0.0047 & 0.0038 & 0.0025 & 0.0013 & 0.0038 & 0.0011 \\ 0.0060 & 0.0013 & 0.0013 & 0.0011 & 0.0007 & 0.0004 & 0.0011 & 0.0003 \end{pmatrix}$$

In (2.22), ($\hat{\tau}$ X $\hat{\tau}$') represents the ITT as the transformation matrix $\hat{\tau}$ is entirely composed of integers as seen in (2.20). The element by element multiplication operation with $\hat{Q}$ can be combined with the quantization stage during lossy image compression to simplify the calculation as shown in subsequent Chapter 3.

2.3 Integer Cosine Transform

Discrete cosine transform is one of the widely popular and time tested transforms employed for various applications ranging from compression to spectral analysis because of its capability for high energy compaction. DCT can be deemed as equivalent to discrete Fourier transform (DFT) with real and even functions. In the DCT domain the input sequence is expressed as a sum of

cosine signals at various frequencies. In view of its wide range of applications, there are numerous fast implementations of DCT and its variations.

Lately, integer approximation of DCT, integer Cosine Transform is gaining popularity thanks to its reduced computational complexity and growing relevance of integer transforms in general.

ICT is preferred over DCT for Video compression as the processing needs to be almost real time and the emphasis is more on speed rather than quality of compression [18].

ICT is being used in High Efficiency Video Coding. HEVC provides better video compression performance than H.264/MPEG-4 AVC. The implementation algorithm of ICT used in HEVC is as follows [11]

Forward transform

- The forward transform is specified as a matrix multiplication in two stages
- Matrix multiplication of input 'X' and the base matrix 'V' horizontally ($Y_1 = VX$)
- The resulting transform coefficients are scaled to obtain Y_2

  $y_2 = (y_1 + \text{offset})>>(M-1+(B-8)), \quad \text{offset}=(1<<(M-2+(B-8)))$
- Matrix multiplication of 'Y_2' and the base matrix 'V' vertically ($Y_3 = Y_2V$)
- The resulting transform coefficients are scaled to obtain 'Y' the ICT of input 'X'

  $y = (y_3 + \text{offset})>>(M+6), \quad \text{offset} = (1<<(M+5))$

Inverse transform

- The inverse transform is also specified as a matrix multiplication in two stages
- Matrix multiplication of input 'X' and the base matrix 'V' horizontally ($X_1 = VY$)
- The resulting transform coefficients are scaled as follows to obtain X_2

$x_2 = (x_1 + \text{offset})>>7$ offset = 1<<(7-1)

- Matrix multiplication of input 'X_2' and the base matrix 'V' vertically ($X_3 = X_2V$)
- The resulting transform coefficients are scaled as follows to obtain the original input X

$X = (x_3 + \text{offset})>>(12-(B-8))$ offset = 1<<(11-(B-8))

The basis vector for input of size 8X8 is given as

$$V = \begin{pmatrix} 64 & 64 & 64 & 64 & 64 & 64 & 64 & 64 \\ 89 & 75 & 50 & 18 & -18 & -50 & -75 & -89 \\ 83 & 36 & -36 & -83 & -83 & -36 & 36 & 83 \\ 75 & -18 & -89 & -50 & 50 & 89 & 18 & -75 \\ 64 & -64 & -64 & 64 & 64 & -64 & -64 & 64 \\ 50 & -89 & 18 & 75 & -75 & -18 & 89 & -50 \\ 36 & -83 & 83 & -36 & -36 & 83 & -83 & 36 \\ 18 & -50 & 75 & -89 & 89 & -75 & 50 & -18 \end{pmatrix}$$

B = internal bit depth (usually '8')

N = transform size (in present case '8')

M = $\log_2 N$ (in present case '3')

The norms of the basis vectors are sufficiently close so that the same scaling can be used for all transform coefficients.

It can be observed that ICT is not a completely faithful adaptation of the DCT as scaling is involved during the estimation process; however, from Section 2.2.1 it can be noticed that there is no approximation involved while developing ITT from DTT. Thus, it is of interest to compare the compression performance of ITT and ICT for various images and identify cases where ITT is a better choice.

2.4 Summary

The main aim of the thesis is to identify areas where ITT can be proposed as an alternative to ICT for image compression. This chapter started off by stating the significance of transform functions in digital signal processing along with the use of polynomial theory in developing these transforms. Then, discrete Tchebichef polynomial was introduced by giving its definition and some of its important properties. Subsequently, the derivation of the corresponding transform, DTT, from the polynomial, DTP, was provided. Further, an integer version (ITT) of the DTT was presented. Using this information, the ITT transformation matrix of size 8X8 was deduced along with normalization matrix involved. Finally, an implementation of ICT used in HEVC which is comparable to that of ITT was introduced.

The next chapter deals with the comparison of performance of a compression algorithm using the ITT and ICT discussed in the current chapter.

Chapter 3

ITT and ICT based Compression

3.1 Multiplier free ITT implementation

In Chapter 2, the expression for ITT was established and the corresponding transformation matrix '$\hat{\tau}$' is derived as shown in (2.19). Though all the elements of the transformation matrix '$\hat{\tau}$' are integers, the matrix multiplication with the input must be carried out in a manner as computationally less intensive as possible. So designing an optimized approach for implementing the transform multiplication is crucial in reducing the computational complexity of the operation. The 1D ITT of input 'X' can be given by ($\hat{\tau}X$). The elements of matrix '$\hat{\tau}$' for size N = 8 are deduced in (2.20). The corresponding 1D transformation Y for an input X of size 8 can be obtained by following the steps shown in Table 3.1.

It can be observed that the process is carried out predominantly by add and subtract operations, thereby reducing the number of multiplication operations which are computationally more intensive. The only multiplying coefficients that appear in the proposed implementation are 2, 3, 4, 6 and 8. The computational complexity can be further decreased by realizing the remaining multiplication operations by a series of shift and add operations as shown in Table 3.2.

Fig. 3.1 shows a 5-stage architectural structure for ID ITT designed following the multiplier-free implementation described in this Section.

Table 3.1: 1D Multiplier free fast ITT

Step 1	$u_o = x_0 + x_7$	$v_o = x_0 - x_7$
	$u_1 = x_1 + x_6$	$v_1 = x_1 - x_6$
	$u_2 = x_2 + x_5$	$v_2 = x_2 - x_5$
	$u_3 = x_3 + x_4$	$v_3 = x_3 - x_4$
Step 2	$k_o = u_0 + u_2$	$z_o = v_0 + v_3$
	$k_1 = u_1 + u_3$	$z_1 = v_1 - v_2$
	$k_2 = u_1 - u_3$	$z_2 = v_1 + v_2$
	$z_4 = 3(v_2 - 3v_3)$	$z_3 = v_1 - v_3$
Step 3	$m_o = k_0 + k_1$	$w_0 = -(z_1 + z_0)$
	$m_1 = k_0 - k_1$	$w_1 = -(z_0 + z_2)$
	$m_2 = 2(3u_0 - 2u_2)$	$w_2 = z_0 - z_2$
	$m_3 = k_0 - k_2$	$w_3 = 2z_1 - z_4$
Step 4	$l_0 = m_0 + m_2$	$l_5 = 2(2v_3 + 3z_2)$
	$l_1 = m_3 + m_2$	$l_6 = 8(2z_1 - z_0 + z_3)$
	$l_2 = 4(2k_2 + u_1)$	
	$l_3 = 4(2u_2 - k_1)$	
	$l_4 = w_0 - 6v_0$	
Step 5	$y_0 = m_0$	$y_4 = l_1 - l_2$
	$y_1 = l_4 - 4z_2$	$y_5 = l_6 + w_2$
	$y_2 = l_0 - 6u_3$	$y_6 = m_1 + l_3$
	$y_3 = l_4 + l_5$	$y_7 = w_1 + 4w_3$

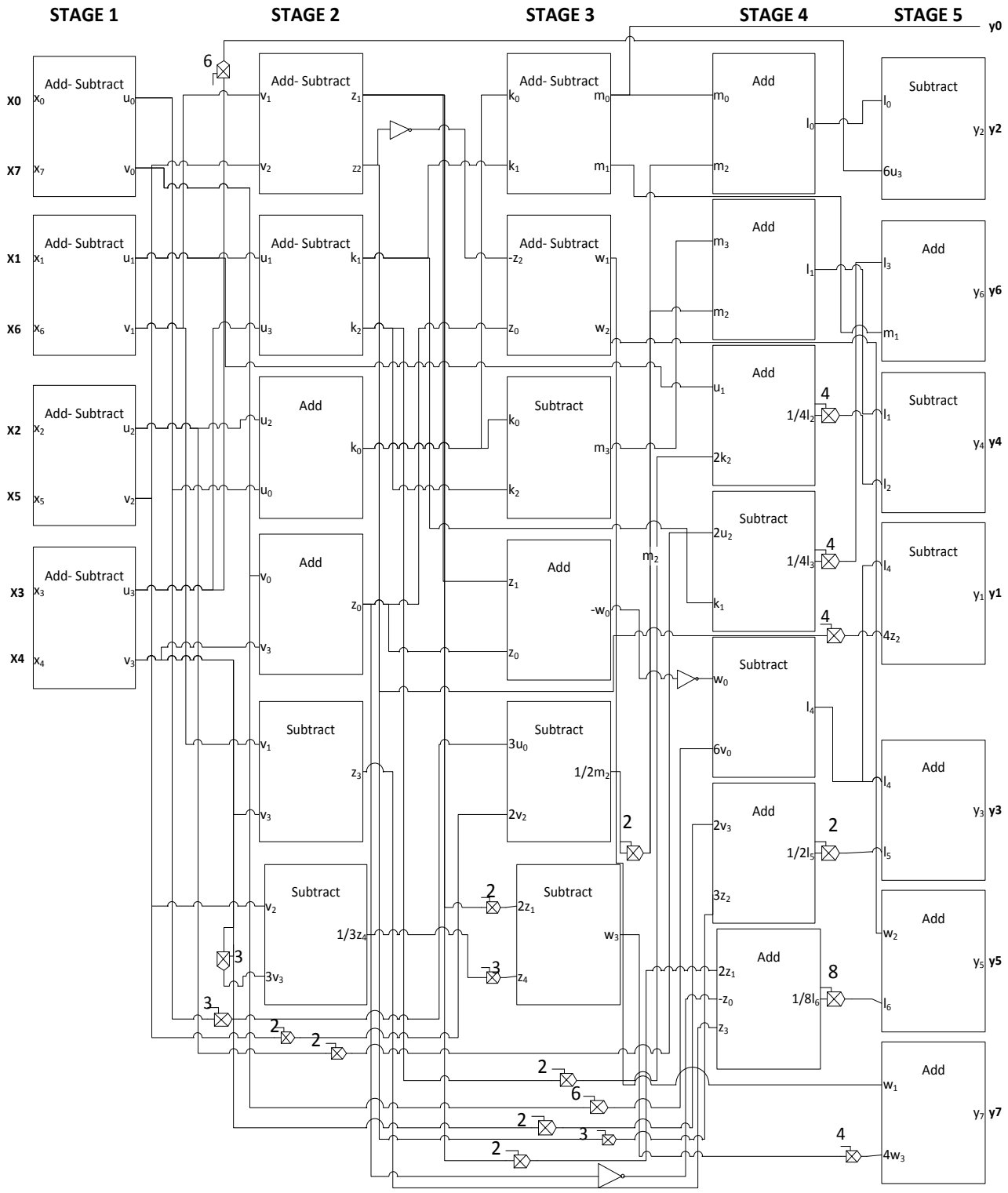

Figure 3.1: Architectural diagram of 1-D Integer DTT

Table 3.2: Multiplication through shift and add operations

$a\times2$ =	$a\times2$ =	*Left shift 'a' by one bit*	= <<a
$a\times3$ =	$(a\times2)+a$ =	*Left shift 'a' by one bit and add 'a' to result*	= (<<a) + a
$a\times4$ =	$(a\times2)\times2$ =	*Left shift 'a' by two bits*	= <<(<< a)
$a\times6$ =	$((a\times2)+a)\times2$ =	*Left shift 'a' by two bits, add 'a' to result and left shift the result by one bit*	= <<(<< a + a)
$a\times8$ =	$((a\times2)\times2))\times2$ =	*Left shift 'a' by three bits*	= <<(<<(<< a))

The 2-D DTT can be computed efficiently by using the proposed 1-D implementation first along the rows and then along the columns in two steps by using the separability property of the DTT as shown below.

$$\hat{\tau}\, X\hat{\tau}' = (\hat{\tau}(\hat{\tau}\, X)')' \qquad (3.1)$$

The block diagram in Fig. 3.2 illustrates the realization of 2D ITT using 1D ITT blocks.

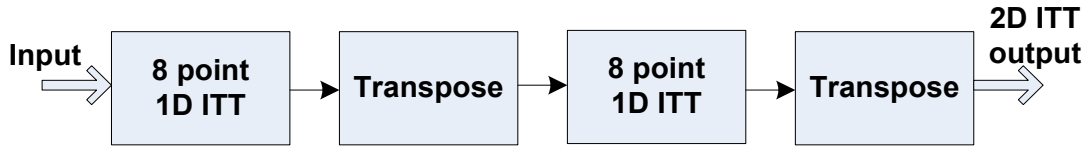

Figure 3.2: 2D ITT implementation using 1D ITT

The element-by-element multiplication between the ITT, namely, $(\hat{\tau}\, X\, \hat{\tau}')$ and factorization matrix $\widehat{Q}$ in (2.23), is incorporated into the quantization stage.

Table 3.3 gives a comparison of the arithmetic complexity of the proposed fast ITT with those for the fast DCTs in [6]–[8] and ICT in [11]. A fast implementation for ITT of size 8×8 does not

exist in the literature though there are non-integer DTT implementations; a comparison of the computational complexity of the proposed ITT is carried out with that of the DCT and ICT.

Table 3.3: Comparison of Computational Complexity

Input type	**Operation**	**DCT[6]**	**DCT[7]**	**DCT[8]**	**ICT[11]**	**ITT**
8 Point 1D array	Add	NA	28	29	NA	44
	Multiply	NA	11	5	NA	0
	Shift	NA	NA	NA	NA	29
8 Point 2D array	Add	454	448	464	448	704
	Multiply	94	176	144	352	0
	Shift	6	NA	NA	128	464

The crucial observation of the comparison in Table 3.3 is that the computationally intensive multiplication operations are completely eliminated by using the proposed ITT implementation for both 1D and 2D cases. There is a minor increase in the number of addition operations for ITT when compared to the rest of the approaches. Additionally, ITT employs shift operations which are not used by the other implementations. The nominal increase in complexity arising from increase in the number of addition and shift operations for ITT is justified by the elimination of multiplication operations which consume more resources.

3.2 Compression and Decompression schemes

For the purpose of comparison between ITT and ICT, compression and decompression of image blocks of size 8×8 are carried out using a scheme similar to the one followed by Joint Photographic Expert Group (JPEG) format [19] as shown in Fig. 3.3 and Fig. 3.4, respectively.

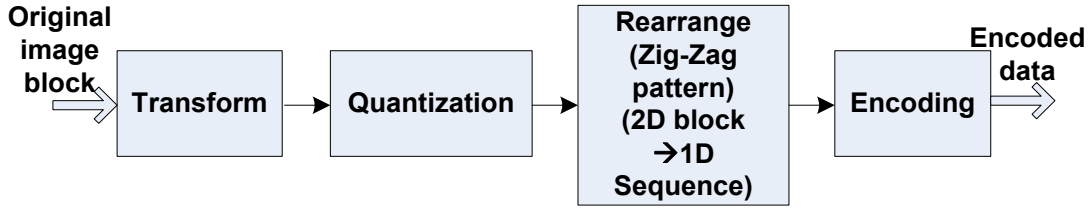

Figure 3.3: Compression scheme

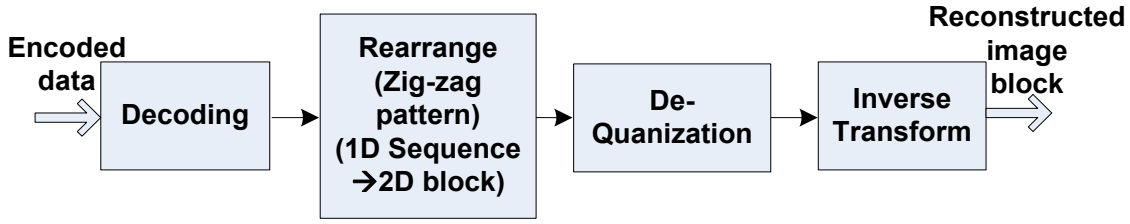

Figure 3.4: Decompression scheme

3.2.1 Compression scheme

The input image is divided into a collection of suitable sized blocks.

Each of the blocks in the compression scheme of Fig. 3.3 is described below.

A. Transformation

Each block undergoes ITT or ICT transformations, as stated in Sections 2.2.1 and 2.3, respectively. Due to the high energy packing efficiencies of ITT and ICT, most of the elements in the higher places are almost zeros in both the cases after transformation. In the case of ITT the factorization with $\widehat{\boldsymbol{Q}}$ is combined with the quantization process.

B. Quantization

The result of the transformation matrix is then subjected to quantization to further increase the amount of compression achieved in lossy compression. During this stage, the transformed input blocks undergo element by element division with a multiple of the standard matrix given below in (3.2) and rounded off to the nearest integer. The multiple is decided based on the amount of compression required.

$$\boldsymbol{Quant} = \begin{bmatrix} \mathbf{16} & \mathbf{11} & \mathbf{10} & \mathbf{16} & \mathbf{24} & \mathbf{40} & \mathbf{51} & \mathbf{61} \\ \mathbf{12} & \mathbf{12} & \mathbf{14} & \mathbf{19} & \mathbf{26} & \mathbf{58} & \mathbf{60} & \mathbf{55} \\ \mathbf{14} & \mathbf{13} & \mathbf{16} & \mathbf{24} & \mathbf{40} & \mathbf{57} & \mathbf{69} & \mathbf{56} \\ \mathbf{14} & \mathbf{17} & \mathbf{22} & \mathbf{29} & \mathbf{51} & \mathbf{87} & \mathbf{80} & \mathbf{62} \\ \mathbf{18} & \mathbf{22} & \mathbf{37} & \mathbf{56} & \mathbf{68} & \mathbf{109} & \mathbf{103} & \mathbf{77} \\ \mathbf{24} & \mathbf{35} & \mathbf{55} & \mathbf{64} & \mathbf{81} & \mathbf{104} & \mathbf{113} & \mathbf{92} \\ \mathbf{49} & \mathbf{64} & \mathbf{78} & \mathbf{87} & \mathbf{103} & \mathbf{121} & \mathbf{120} & \mathbf{101} \\ \mathbf{72} & \mathbf{92} & \mathbf{95} & \mathbf{98} & \mathbf{112} & \mathbf{100} & \mathbf{103} & \mathbf{99} \end{bmatrix} \quad (3.2)$$

It can be observed that the quantization matrix elements are in an almost ascending order, as it is traversed from left to right and top to bottom. As a result, after the operation, more elements in the quantized transformed block are set to zero. At the end of quantization, the smaller frequency components which are located at the top left corner preserve their accuracies better than the larger frequency components of the image. Depending upon the level of compression desired, the fixed quantization matrix (3.2) is multiplied by a quantization factor. Higher the quantization factor, higher is the amount of compression achieved. The quantization process is dealt more in detail while discussing the variable quantization based compression technique in Chapter 4.

C. Rearrangement

The ensuing quantized matrix is then converted into a 1D sequence by reading the matrix in a zig-zag fashion as shown in Fig. 3.5 for an 8×8 matrix.

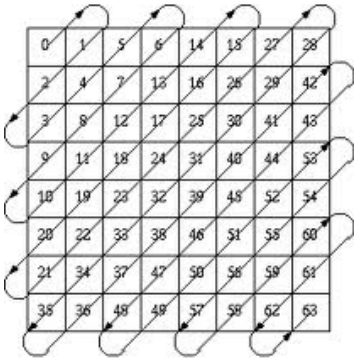

Figure 3.5: Zig-Zag read

D. Encoding

The resultant sequence then undergoes encoding to reduce the amount of information to be transmitted. Usually, run length encoding (RLE) is employed to reduce the amount of information being transmitted due to the presence of series of zeros in the sequence. This can be followed by any other encoding technique to further condense the data to be transmitted.

The final encoded sequence is transmitted over a channel to the receiver where it is converted back into an image by following the process shown in Fig. 3.4.

3.2.2 De-Compression scheme

The received sequence is decoded before arranging it back into a matrix following the same zig-zag fashion employed for reading the matrix during compression. The resulting matrix is then de-quantized by multiplying it with the same quantization matrix that was used during the quantization process. The ensuing result might not be exactly the same as the input to the quantization process due to loss of precision, thereby affecting the quality of the final image. Finally, the de-quantized matrix is subjected to inverse transform to complete the decompression process. The collection of all such decompressed image blocks gives the required reconstructed

image. Ideally, the reconstructed image must be an exact replica of the image before compression. This might not be possible due to loss of precision during quantization, because of which the decompressed image is expected to be just as close to the original uncompressed image as possible.

The quality of the reconstructed image is based on its similarity to the original image before compression. The compression efficiency on the other hand is estimated considering the size of the encoded data after compression and the size of the original image. These aspects can be explained using the various measures discussed in Section 3.3.

3.3 Evaluation Parameters

3.3.1 Picture Characterization

All images are not created equal. The quality of compression achieved for an image depends as much on its spatial and frequency content as on the technique adopted for compression. Measures like s*pectral activity measure* ***(SAM)*** and *spatial frequency measure* ***(SFM)*** are employed to assess the structural nature of the image [20]. SAM gives a measure of image predictability in the spectral domain, and is defined as the ratio of arithmetic mean to the geometric mean of squared DFT coefficients

It is given by

$$SAM = \frac{\frac{1}{M.N}\sum_{i=0}^{M-1}\sum_{j=0}^{N-1}|F(i,j)|^2}{\left\{\prod_{i=0}^{M-1}\prod_{j=0}^{N-1}|F(i,j)|^2\right\}^{\frac{1}{M.N}}} \qquad (3.3)$$

where M and N are the numbers of pixels in the horizontal and vertical directions and $F(i, j)$ is the $(i,j)^{th}$ DFT coefficient of the original image.

SAM of an image is directly proportional to the predictability of the image and has a dynamic range of $[1, \infty)$.

SFM on the other hand indicates the overall activity level in a picture, defined by the *row frequency*, R_f and the *column frequency*, C_f.

It is given by

$$SFM = \sqrt{{R_f}^2 + {C_f}^2} \qquad (3.4)$$

$$R_f = \sqrt{\frac{1}{M.N}\sum_{i=1}^{M}\sum_{j=2}^{N}\left(x_{i,j} - x_{i,(j-1)}\right)^2} \qquad (3.5)$$

$$C_f = \sqrt{\frac{1}{M.N}\sum_{j=1}^{M}\sum_{i=2}^{N}\left(x_{i,j} - x_{(i-1),j}\right)^2} \qquad (3.6)$$

where, x_{ij} represents the $(i,j)^{th}$ pixel value of the original image and M and N are the numbers of pixels in the horizontal and vertical directions. SFM is directly proportional to the number of high frequency components in the image.

In general, images with a large SFM and a small SAM (closer to unity) are difficult to code, since they have high frequency content and are not very predictable. SFM and SAM together make it possible to assess the performance of a discrete transform on different images.

3.3.2 Picture quality evaluation

Picture quality evaluation (PQE) measures can be subjective or objective [21]. While subjective measures are based on the psycho-visual physics of human perception, objective measures deal with distortions that a human eye cannot capture. In [22], [23], the authors have proposed a set of quality parameters composed of objective measurements which are as follows.

i. *Normalized cross-correlation (**NK**)* –Depiction of the cross-correlation between the original and reconstructed images, normalized with respect to the original image.

$$NK = \frac{\sum_{i=1}^{M}\sum_{j=1}^{N} x_{i,j}x'_{i,j}}{\sum_{i=1}^{M}\sum_{j=1}^{N}(x_{i,j})^2} \quad (3.7)$$

where M is the number of rows in the image, N is the number of columns in the image, $x_{i,j}$ represents the (i,j)th pixel value of the original image, and $x'_{i,j}$ the (i,j)th pixel value of the reconstructed image

The reconstructed image must be as close to the original image as possible and as a result the value of NK would be around unity.

ii. *Structural content (**SC**)* – Comparative measure of the structural content between the original and the reconstructed image after compression. It is given by the ratio of sum of squared pixel values of the original image to that of the reconstructed image.

$$SC = \frac{\sum_{i=1}^{M}\sum_{j=1}^{N}(x_{i,j})^2}{\sum_{i=1}^{M}\sum_{j=1}^{N}(x'_{i,j})^2} \quad (3.8)$$

If the reconstructed image is a close approximate of the original, then the value of SC would be close to unity.

iii. *Average difference (**AD**)*–An average of the difference between the original and the reconstructed image after compression in the range [0, maximum possible pixel intensity]. It is given by the ratio of the sum of the pixel difference between the original and reconstructed images to the number of pixels in the image.

$$AD = \frac{1}{MN}\sum_{i=1}^{M}\sum_{j=1}^{N}\left|x_{i,j} - x'_{i,j}\right| \quad (3.9)$$

AD value must be as low as possible to indicate that difference between the original and reconstructed image is nominal.

iv. *Maximum difference (**MD**)* – Maximum difference between corresponding pixel values of the original and reconstructed images in the range [0, maximum possible pixel intensity].

$$MD = max(\left|x_{i,j} - x'_{i,j}\right|) \quad (3.10)$$

Though MD might be large due to a random pixel discrepancy, it is still possible for the overall image to have a faithful reconstruction.

v. *Laplacian mean squared error (**LMSE**)* – Classifies the edge information, which impinges heavily on the human perception of the image and is given by

$$LMSE = \frac{\sum_{i=1}^{M}\sum_{j=1}^{N}\left(x_{i,j} - x'_{i,j}\right)^2}{\sum_{i=1}^{M}\sum_{j=1}^{N}\left(x_{i,j}\right)^2} \quad (3.11)$$

Ideally the value of LMSE must be zero. LMSE is worse when the reconstructed image is over approximated for majority of the pixels.

vi. *Normalized absolute error (**NAE**)* – Represents the mean absolute error, normalized with respect to the original image.

$$NAE = \frac{\sum_{i=1}^{M}\sum_{j=1}^{N}|x_{i,j} - x'_{i,j}|}{\sum_{i=1}^{M}\sum_{j=1}^{N}|x_{i,j}|} \quad (3.12)$$

Ideally when the reconstructed image is a close replica of the input image before compression, the correlation-based measures (NK, SC) should be close to unity, whereas, the Human Visual System (HVS)-based measures (NAE, LMSE) and the difference-based measures (AD, MD) should be close to zero.

3.3.3 Performance Curves

Compression techniques can be rated based on predominantly two factors:

- The reduction in size of data after compression and
- Similarity between the original image and the reconstructed image at the receiver after decompression

In order to rate the performance of different compression techniques, the compression performance curves are plotted between suitable evaluation parameters.

RMSE vs. CR

- RMSE (*Root mean square error*) is a measure of the amount of deviation of the reconstructed image from the uncompressed image. Higher the RMSE, higher is the deviation.

$$RMSE = \sqrt{\frac{1}{M.N}\sum_{i=1}^{M}\sum_{j=2}^{N}\left(x_{i,j} - x'_{i,j}\right)^2}$$

where, x_{ij}, x'_{ij} represent the $(i,j)^{th}$ pixel value of the original and reconstructed images. Whereas, *M* and *N* are the number of pixels in the horizontal and vertical directions of the image.

- CR (*Compression ratio*) is the measure of the amount of compression the image has undergone. Higher the CR, higher is the amount of compression achieved.

$$CR = \frac{Size\ of\ uncompressed\ image}{Size\ of\ compressed\ image}$$

- The performance curve is plotted with RMSE as a function of CR. As the aim of compression is to have as low deviation from the original as possible at as high a compression level as possible, it is preferred to have a low RMSE and a high CR.
- Lower the performance curve, better is the compression performance

PSNR vs. bpp:

- PSNR (*Peak signal to noise ratio*) is widely employed to evaluate the image reconstruction quality during compression. Higher the PSNR better is the quality of image.

$$PSNR = 20\log_{10} 255/RMSE$$

where, '255' is the maximum intensity possible in the image

- Bpp (*Bits per pixel*) is a measure of the amount of compression the image has undergone. It is the average number of bits per pixel used for representing the image after compression.

$$bpp = \frac{No.of\ bits\ used\ for\ transmitting\ the\ compressed\ image}{No.of\ pixels\ in\ the\ image}$$

Lower the bpp, higher is the amount of compression achieved.

- The performance curve is plotted with PSNR as a function of bpp. As the aim of compression is to achieve high image quality with less data to represent the image, it is preferred to have a high PSNR and a low bpp.
- Higher the performance curve, better is the compression performance

3.4 Simulation

MATLAB [24] software is chosen to simulate the image compression scheme described in Section 3.2 using both ITT and ICT. A variety of input images are selected to analyze and compare the compression results obtained using the two transforms. These images differ in the type of content and their amount of detail, which is indicated by the values of SAM and SFM parameters. Each of these images is subjected to compression and decompression according to the schemes presented in Section 3.2.

The level of compression of the image is varied by adjusting the factor multiplying the quantization matrix (3.2) used during the quantization phase of the compression. If the factor is high, the quality of the compression decreases, whereas amount of compression increases. In the current simulation a user defined input parameter 'Quality', specified as a positive integer in the range [1,100], determines the quantization factor to be used during compression. The relationship between the quantization factor and 'Quality' is given as

$$\boldsymbol{Quantization\ factor} = \begin{cases} \mathbf{50}/\boldsymbol{Quality} & \boldsymbol{Quality} \leq \mathbf{50} \\ (\mathbf{100} - \boldsymbol{Quality})/\mathbf{50} & \mathbf{50} < Quality \leq 100 \end{cases} \quad (3.5)$$

If 'Quality' is 100, the quantization factor is zero and the process is carried without any quantization, leading to non-lossy compression. Similarly, if 'Quality' is set to 50 the image is

quantized with the exact matrix in (3.2). By varying the quality parameter, the image is subjected to different levels of compression. The PQE measures as well as the performance evaluation measures discussed in Sections 3.3.2 and 3.3.3, respectively, are calculated at each level of compression. Using the results, the performance plots of PSNR vs. bpp and RMSE vs. CR along with the PQE measures (Table 3.4 - Table 3.10) are obtained for each of the input images. In the performance plots, the curves in blue pertain to compression using ITT, whereas the curves in red represent ICT-based compression.

3.4.1 Lena Image

Lena [25] in Fig. 3.6 is one of the most widely used images in image processing. The input image used is of size 512×512 pixels. The image characterization parameters SAM and SFM are given as 323.348 and 14.3292, respectively. The moderate SAM indicates medium predictability of the image along with considerable amount of spectral activity.

Figure 3.6: Lena [25]

The image is subjected to compression and subsequent decompression for a chosen range of compression quality levels. The quality level can be varied as explained above by varying the

factor that multiplies the quantization matrix. At each level, the reconstructed image is compared with the original uncompressed image and the parameters discussed in Section 3.3 are calculated and tabulated (see Table 3.4). The performance curves, RMSE vs. CR as well as PSNR vs. bpp, are shown in Fig. 3.7 and Fig. 3.8, respectively, using the data in Table 3.4.

Table 3.4: Quality Measures for 8X8 Image Compression of the Lena image

Quality	5	10	15	30	35	40	45	60	65	80	85
ITT											
RMSE	11.14	7.80	6.49	4.95	4.68	4.48	4.30	3.85	3.68	3.04	2.72
PSNR	27.16	30.25	31.85	34.20	34.69	35.06	35.43	36.39	36.78	38.43	39.39
bpp	0.58	0.83	1.04	1.53	1.67	1.80	1.93	2.35	2.55	3.51	4.15
CR	13.70	9.69	7.72	5.22	4.78	4.46	4.14	3.40	3.14	2.28	1.93
NK	1.00	1.00	1.00	1.00	1.00	1.00	1.00	1.00	1.00	1.00	1.00
SC	1.00	1.00	1.00	1.00	1.00	1.00	1.00	1.00	1.00	1.00	1.00
NAE	0.07	0.04	0.04	0.03	0.03	0.03	0.02	0.02	0.02	0.02	0.02
LMSE	0.01	0.00	0.00	0.00	0.00	0.00	0.00	0.00	0.00	0.00	0.00
AD	8.35	5.67	4.69	3.58	3.39	3.26	3.12	2.80	2.68	2.22	2.00
MD	110	84	75	58	63	66	44	41	38	24	22
ICT											
RMSE	11.04	7.64	6.34	4.82	4.56	4.38	4.20	3.77	3.60	3.01	2.72
PSNR	27.23	30.44	32.05	34.43	34.91	35.27	35.64	36.57	36.97	38.52	39.41
bpp	0.58	0.82	1.03	1.53	1.67	1.80	1.94	2.35	2.56	3.50	4.15
CR	13.68	9.72	7.77	5.23	4.78	4.46	4.13	3.40	3.13	2.28	1.93
NK	1.00	1.00	1.00	1.00	1.00	1.00	1.00	1.00	1.00	1.00	1.00
SC	0.99	0.99	0.99	0.99	0.99	0.99	0.99	0.99	0.99	0.99	0.99
NAE	0.07	0.04	0.04	0.03	0.03	0.03	0.02	0.02	0.02	0.02	0.02
LMSE	0.01	0.00	0.00	0.00	0.00	0.00	0.00	0.00	0.00	0.00	0.00
AD	8.34	5.61	4.65	3.54	3.35	3.23	3.09	2.78	2.66	2.24	2.03
MD	94	68	58	50	53	56	54	46	37	33	19

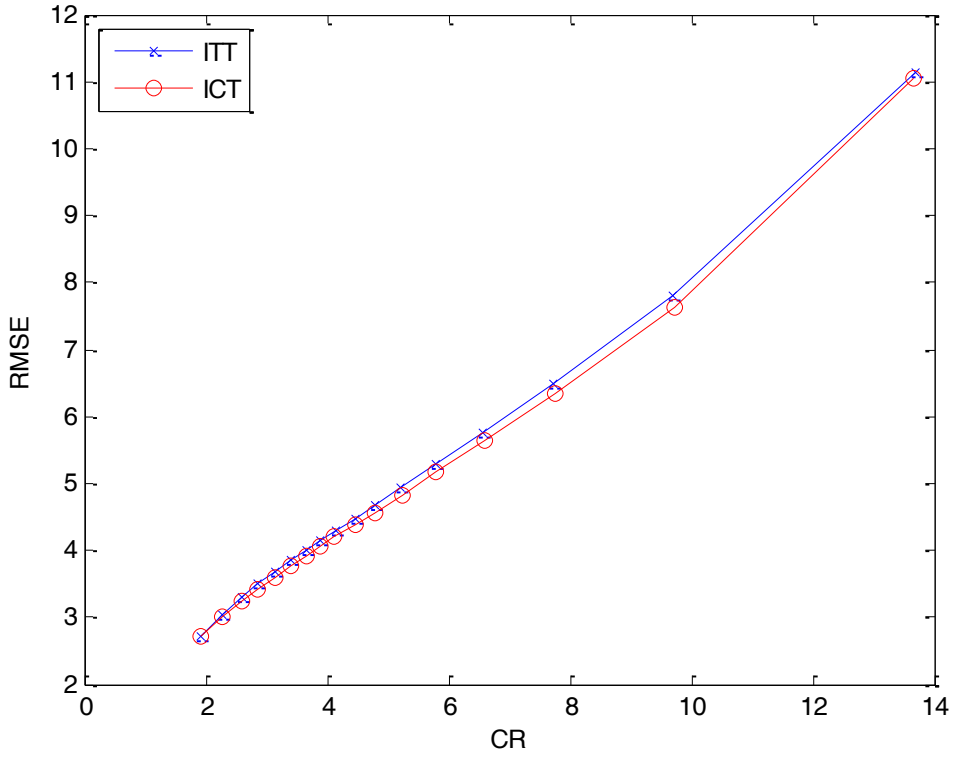

Figure 3.7: RMSE vs. CR plot for 8X8 compression of the Lena image

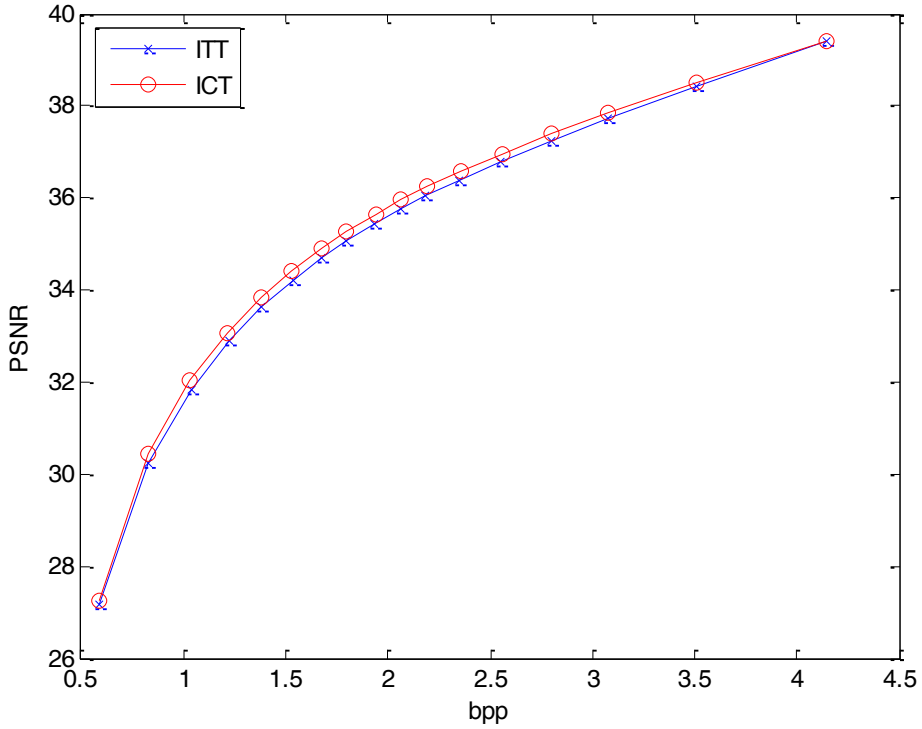

Figure 3.8: PSNR vs. bpp plot for 8X8 compression of the Lena image

It can be observed from the tabulated results that as the 'Quality' parameter of the compression improves, the PSNR increases, RMSE decreases, correlation-based parameters approach unity, and the difference and HVS-based parameters approach zero for both the ITT-and ICT-based compression. But at the same time, the amount of compression decreases and the number of bits needed to represent the compressed image increases due to a raise in the precision of data. From Fig. 3.7, it is obvious that CR and RMSE are almost proportional to each other. From Fig. 3.8, it can be noticed that the PSNR also increases as bpp increases. By comparing the PQE measures in Table 3.4, it can be deduced that the performance of ITT is very close to that of ICT owing to the nominal difference in the values for all the ten parameters listed. Moreover, as the PSNR and RMSE plots of ITT are almost overlapping with those of ICT, it can be stated that ITT and ICT offer comparable performance in case of images with medium SAM.

3.4.2 Jupiter Image

Fig. 3.9 shows an image of the Jupiter planet, along with its satellite, taken from space by NASA. The image of the planet Jupiter of size 308×256 has been procured from image database [26]. It has a SAM and SFM of 1997.9 and 6.4426, respectively. So it can be concluded that the image is moderately predictive.

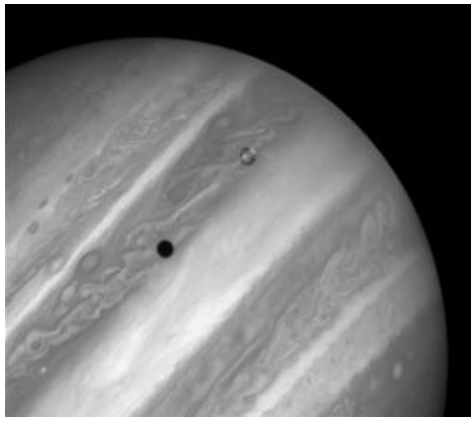

Figure 3.9: Jupiter [26]

The image is subjected to compression and decompression using both ITT-and ICT-based approaches for a range of compression levels, as described in Section 3.4.1. The PQE measures as well as the performance parameters are calculated at each level of compression and are consolidated in Table 3.5. Fig. 3.10 and Fig. 3.11 depict the performance curves for the image compression plotted using the data thus obtained.

Table 3.5: Quality Measures for 8X8 Image Compression of the Jupiter image

Quality	5	10	15	30	35	40	45	60	65	80	85
ITT											
RMSE	9.05	5.48	4.40	2.94	2.72	2.62	2.44	1.89	1.68	1.25	1.13
PSNR	28.97	33.32	35.23	38.72	39.40	39.74	40.35	42.55	43.60	46.17	47.00
bpp	0.46	0.61	0.75	1.14	1.18	1.23	1.32	1.87	1.94	2.17	2.33
CR	17.53	13.03	10.71	6.99	6.76	6.51	6.05	4.29	4.13	3.68	3.44
NK	1.00	1.00	1.00	1.00	1.00	1.00	1.00	1.00	1.00	1.00	1.00
SC	1.00	1.00	1.00	1.00	1.00	1.00	1.00	1.00	1.00	1.00	1.00
NAE	0.07	0.03	0.03	0.02	0.02	0.02	0.01	0.01	0.01	0.01	0.01
LMSE	0.00	0.00	0.00	0.00	0.00	0.00	0.00	0.00	0.00	0.00	0.00
AD	7.45	3.65	3.28	1.89	1.74	1.87	1.57	1.17	1.02	0.74	0.67
MD	69	55	52	27	25	22	26	22	20	12	14
ICT											
RMSE	9.18	5.46	4.53	2.89	2.68	2.61	2.51	1.67	1.45	0.98	0.95
PSNR	28.84	33.35	34.98	38.88	39.54	39.75	40.10	43.63	44.85	48.28	48.54
bpp	0.45	0.62	0.73	1.16	1.16	1.16	1.22	2.07	2.08	2.08	2.08
CR	17.59	12.96	10.94	6.90	6.90	6.89	6.56	3.87	3.85	3.85	3.84
NK	1.00	1.00	1.00	1.00	1.00	1.00	1.00	1.00	1.00	1.00	1.00
SC	0.99	0.99	0.99	0.99	0.99	0.99	0.99	0.99	0.99	0.99	0.99
NAE	0.07	0.03	0.03	0.02	0.02	0.02	0.02	0.01	0.01	0.01	0.01
LMSE	0.00	0.00	0.00	0.00	0.00	0.00	0.00	0.00	0.00	0.00	0.00
AD	7.60	3.67	3.53	1.92	1.76	1.92	1.66	1.11	1.09	0.64	0.64
MD	70	50	43	23	20	19	22	15	11	8	7

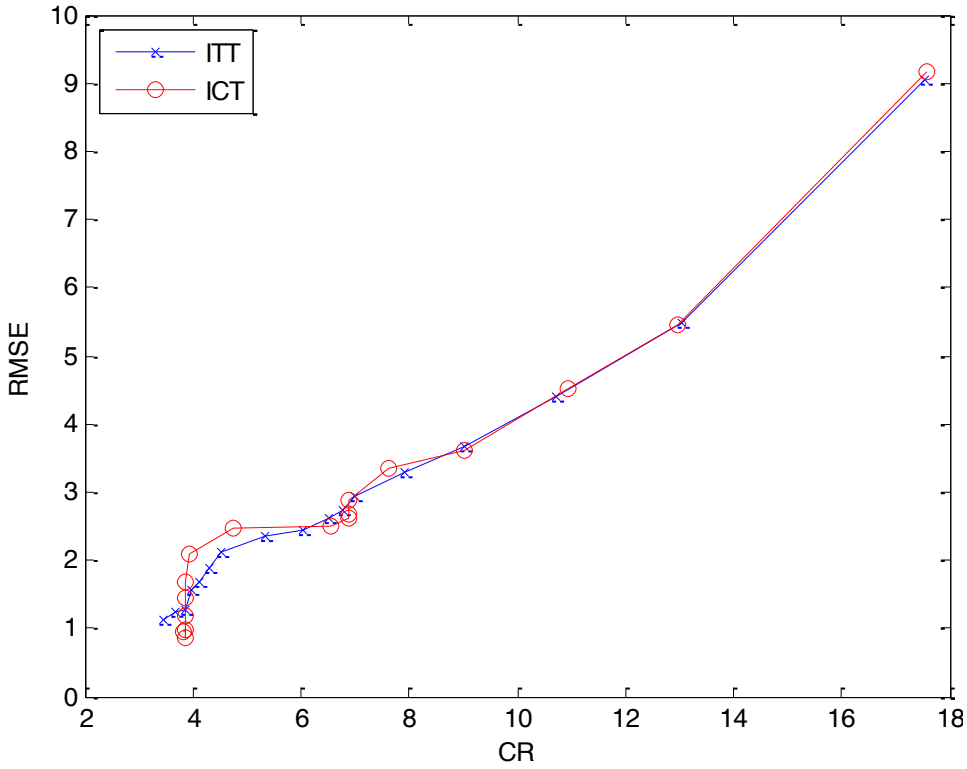

Figure 3.10: RMSE vs. CR plot for 8X8 compression of the Jupiter image

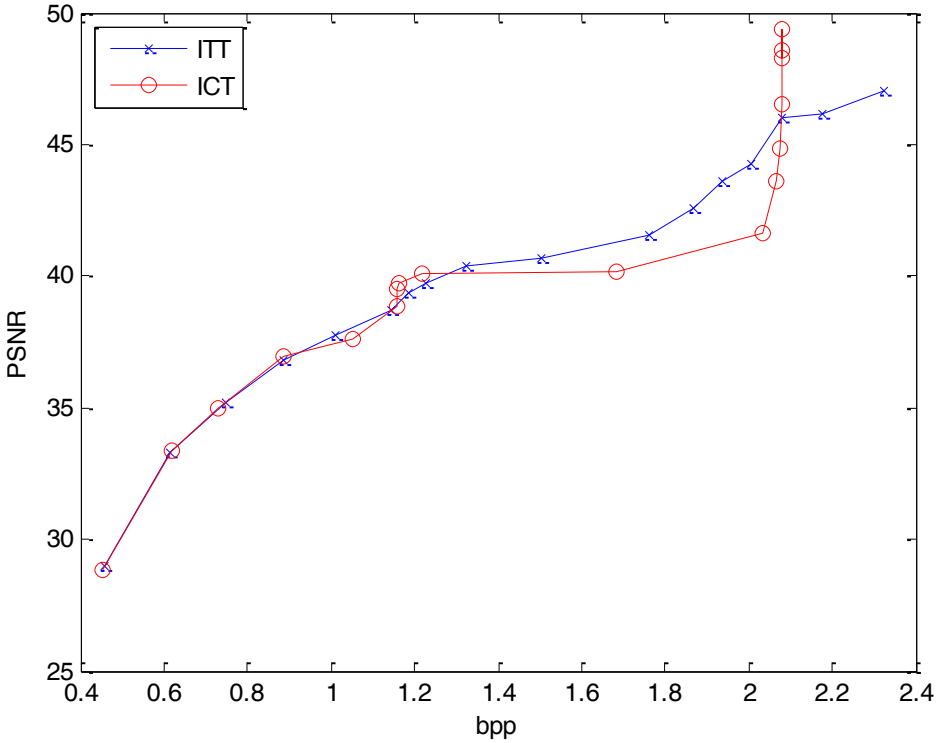

Figure 3.11: PSNR vs. bpp plot for 8X8 compression of the Jupiter image

It can be deduced from the Table 3.5 that the relation between the various image parameters remains the same as described in Section 3.4.1. The reconstructed image is still faithful enough to the original in all the cases, as the correlation-based parameters NK and SC are unity and the HVS-based parameters NAE and LMSE are zero. The parameters AD and MD are also nominal at low quality compression and decrease further in value as the quality is increased. The difference between the various parameters for ITT and ICT listed in Table 3.5 is still not too large. From Fig. 3.10 the RMSE vs. CR curves for ITT and ICT are almost overlapping. Their PSNR vs. bpp curves can be termed as close to each other on the whole as can be noted from Fig. 3.11. It can also be noticed that PSNR of ICT slightly falls below that of ITT for bpp higher than 1.4. Thus it can be stated that ITT and ICT offer similar compression performances for images with moderate predictability.

3.4.3 Cameraman Image

Cameraman image in Fig. 3.12 of '.tif' format is another classic image that is widely used in image processing. The size of the image is 512×512 and is sourced from [25]. The corresponding SAM and SFM values are 1794.7 and 14.3603, respectively. From the high SAM value, it can be inferred that the image is highly predictive.

Figure 3.12: Cameraman [25]

After the image is compressed and subsequently decompressed using ITT-and ICT-based compression techniques presented in Section 3.2, the various compression and quality parameters listed in Section 3.3 are calculated by comparing the final reconstructed and the uncompressed images. The same is repeated for various compression levels by varying the user defined quality parameter as defined in Section 3.4 and tabulated in Table 3.6 and the corresponding performance plots are presented in Fig. 3.13 and Fig. 3.14.

Table 3.6: Quality Measures for 8X8 Image Compression of the Cameraman image

Quality	5	10	15	30	35	40	45	60	65	80	85
ITT											
RMSE	10.53	7.16	5.72	4.07	3.76	3.53	3.32	2.84	2.65	2.00	1.72
PSNR	27.65	31.00	32.95	35.91	36.60	37.14	37.67	39.03	39.62	42.08	43.39
bpp	0.55	0.76	0.92	1.32	1.44	1.53	1.64	1.95	2.11	2.83	3.29
CR	14.44	10.57	8.66	6.04	5.57	5.23	4.88	4.10	3.80	2.83	2.43
NK	1.00	1.00	1.00	1.00	1.00	1.00	1.00	1.00	1.00	1.00	1.00
SC	0.99	1.00	1.00	1.00	1.00	1.00	1.00	1.00	1.00	1.00	1.00
NAE	0.06	0.04	0.03	0.02	0.02	0.02	0.02	0.02	0.02	0.01	0.01
LMSE	0.01	0.00	0.00	0.00	0.00	0.00	0.00	0.00	0.00	0.00	0.00
AD	7.57	4.99	3.83	2.73	2.52	2.37	2.23	1.91	1.79	1.36	1.17
MD	108	80	67	46	38	39	32	33	25	23	18
ICT											
RMSE	10.31	6.97	5.52	3.88	3.59	3.37	3.17	2.72	2.55	1.97	1.74
PSNR	27.83	31.23	33.26	36.32	37.00	37.55	38.08	39.41	39.97	42.20	43.27
bpp	0.55	0.75	0.92	1.31	1.42	1.52	1.62	1.93	2.08	2.78	3.23
CR	14.47	10.66	8.71	6.11	5.62	5.27	4.93	4.14	3.84	2.87	2.48
NK	1.00	1.00	1.00	1.00	1.00	1.00	1.00	1.00	1.00	1.00	1.00
SC	0.99	0.99	0.99	0.99	0.99	0.99	0.99	0.99	0.99	0.99	0.99
NAE	0.06	0.04	0.03	0.02	0.02	0.02	0.02	0.02	0.02	0.01	0.01
LMSE	0.01	0.00	0.00	0.00	0.00	0.00	0.00	0.00	0.00	0.00	0.00
AD	7.47	4.94	3.82	2.70	2.51	2.36	2.22	1.93	1.81	1.42	1.27
MD	107	73	56	40	34	32	30	32	27	22	14

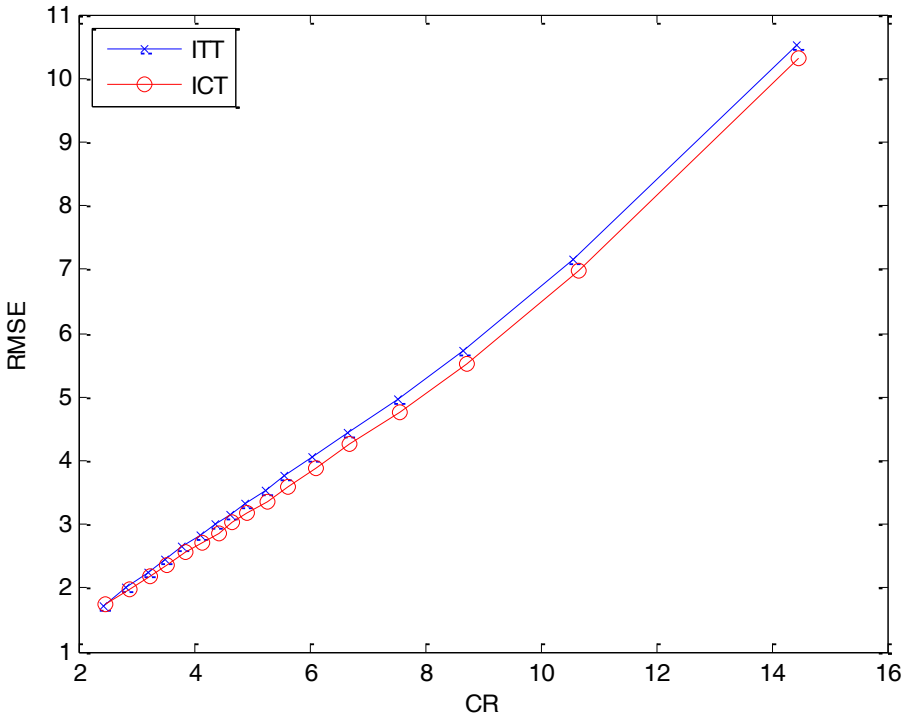

Figure 3.13: RMSE vs. CR plot for 8X8 compression of the Cameraman image

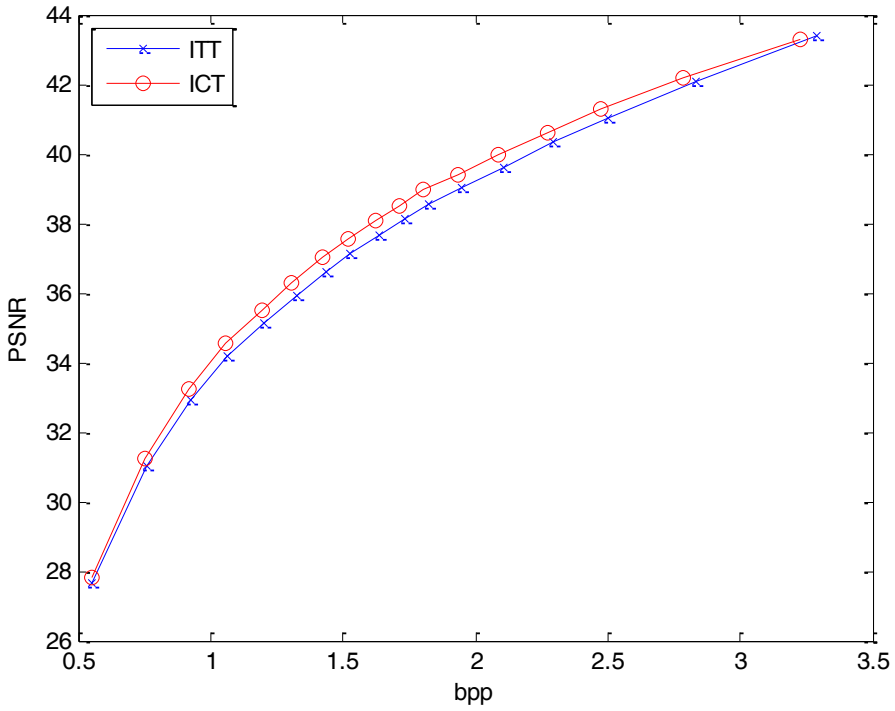

Figure 3.14: PSNR vs. bpp plot for 8X8 compression of the Cameraman image

The RMSE and the PSNR plots in Fig. 3.13 and Fig. 3.14 convey that the performance of ICT is better than that of ITT in this case. At higher compressions, it can be noted from Fig. 3.13 that RMSE of ITT is higher than that with ICT indicating a slightly lesser image quality. It can be observed that ICT offers a marginally higher PSNR than ITT for a fixed value of 'bpp' from Fig. 3.13. The rest of the PQE measures in Table 3.6 are almost same for ITT and ICT, except that the difference parameters, namely, AD and MD of ICT are marginally better than that of ITT. So it can be inferred that ICT offers a slightly better compression performance than ITT.

3.4.4 Assorted Patterns Image

The image shown in Fig. 3.15 [25] is an assorted collection of patterns. This image of size 500×500 contains alphabets of different sizes, granular patches of varying density, sharp edges squares of different sizes, series of parallel bars and circular dots of varying grey level intensity. Its corresponding SAM and SFM values can be given as 19.53 and 63.6, respectively. Thus, the image can be said to be less predictable with considerable spectral content.

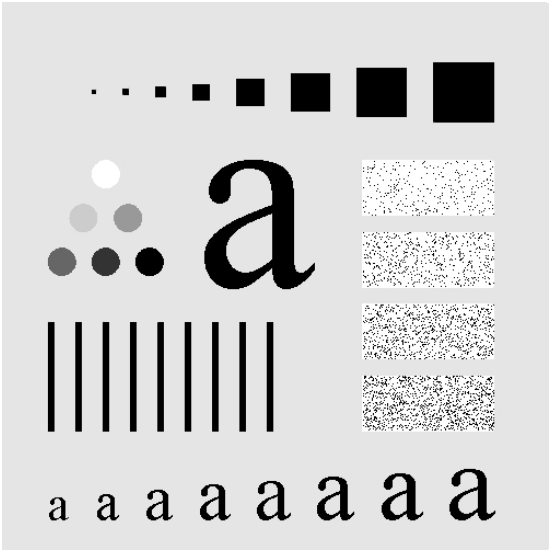

Figure 3.15: Assorted patterns [25]

The image is subjected to compression of varying strength similar to the inputs discussed in the previous Sections 3.4.1 - 3.4.3. Table 3.7 consolidates the various quality parameters of the compression performance using ITT and ICT. The RMSE and PSNR plots in Fig. 3.16 and Fig. 3.17 are drawn based on this data.

Table 3.7: Quality Measures for 8X8 Image Compression of the assorted patterns image

Quality	5	10	15	30	35	40	45	60	65	80	85
ITT											
RMSE	19.06	16.79	14.87	9.45	8.28	7.54	6.76	5.08	4.57	2.64	2.03
PSNR	22.50	23.60	24.65	28.59	29.74	30.55	31.50	33.97	34.90	39.65	41.96
bpp	0.90	1.15	1.35	1.85	1.98	2.08	2.18	2.43	2.52	2.83	2.96
CR	8.90	6.96	5.95	4.33	4.05	3.84	3.68	3.30	3.17	2.82	2.71
NK	0.98	0.99	0.98	0.99	0.99	0.99	1.00	1.00	0.99	1.00	1.00
SC	1.03	1.02	1.03	1.01	1.01	1.02	1.01	1.00	1.01	1.00	1.00
NAE	0.03	0.03	0.03	0.01	0.01	0.01	0.01	0.01	0.01	0.00	0.00
LMSE	0.01	0.01	0.00	0.00	0.00	0.00	0.00	0.00	0.00	0.00	0.00
AD	6.55	5.58	5.50	2.75	2.39	2.96	1.99	1.53	2.04	0.80	0.61
MD	255	246	230	169	143	113	104	69	60	37	28
ICT											
RMSE	19.21	17.11	14.99	9.55	8.35	7.57	6.91	5.17	4.64	2.89	2.27
PSNR	22.43	23.43	24.58	28.50	29.66	30.52	31.31	33.82	34.77	38.87	40.96
bpp	0.90	1.14	1.34	1.86	1.98	2.08	2.17	2.44	2.53	2.85	2.98
CR	8.89	7.00	5.96	4.30	4.03	3.85	3.68	3.28	3.17	2.81	2.68
NK	0.99	0.99	0.99	1.00	1.00	0.99	1.00	1.00	1.00	1.00	1.00
SC	1.02	1.02	1.02	1.00	1.01	1.01	1.00	1.00	1.00	1.00	0.99
NAE	0.03	0.03	0.03	0.02	0.01	0.01	0.01	0.01	0.01	0.01	0.01
LMSE	0.01	0.01	0.00	0.00	0.00	0.00	0.00	0.00	0.00	0.00	0.00
AD	6.19	5.50	5.11	3.52	2.55	2.55	2.74	1.70	1.56	1.55	1.34
MD	255	244	222	161	129	138	116	71	69	34	25

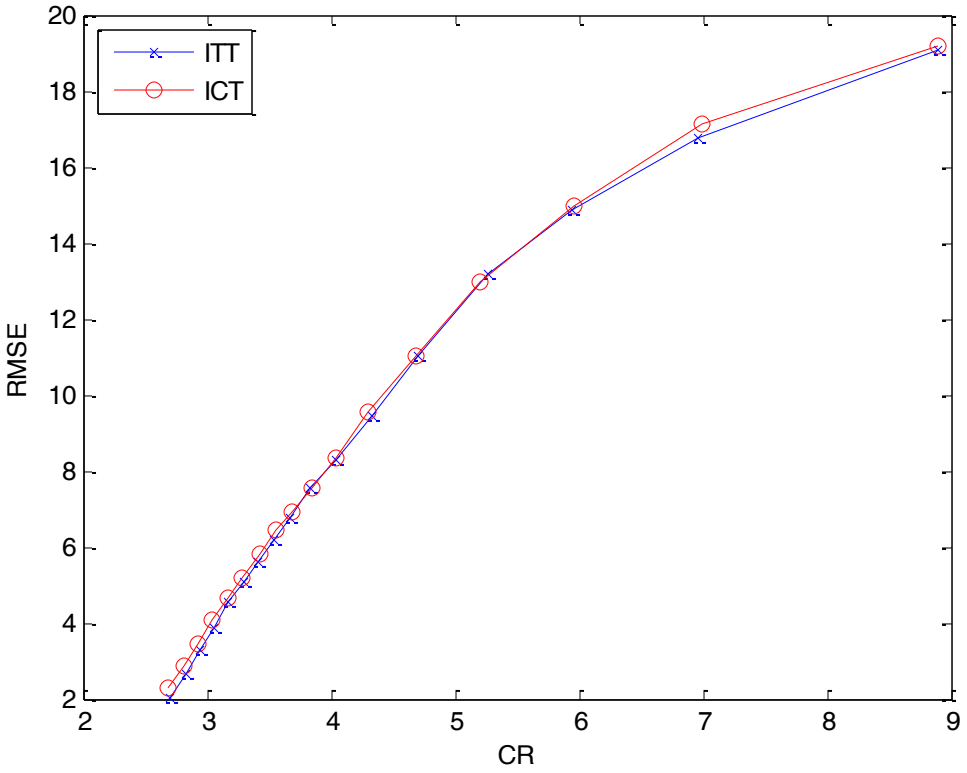

Figure 3.16: RMSE vs. CR plot for 8X8 compression of the assorted patterns image

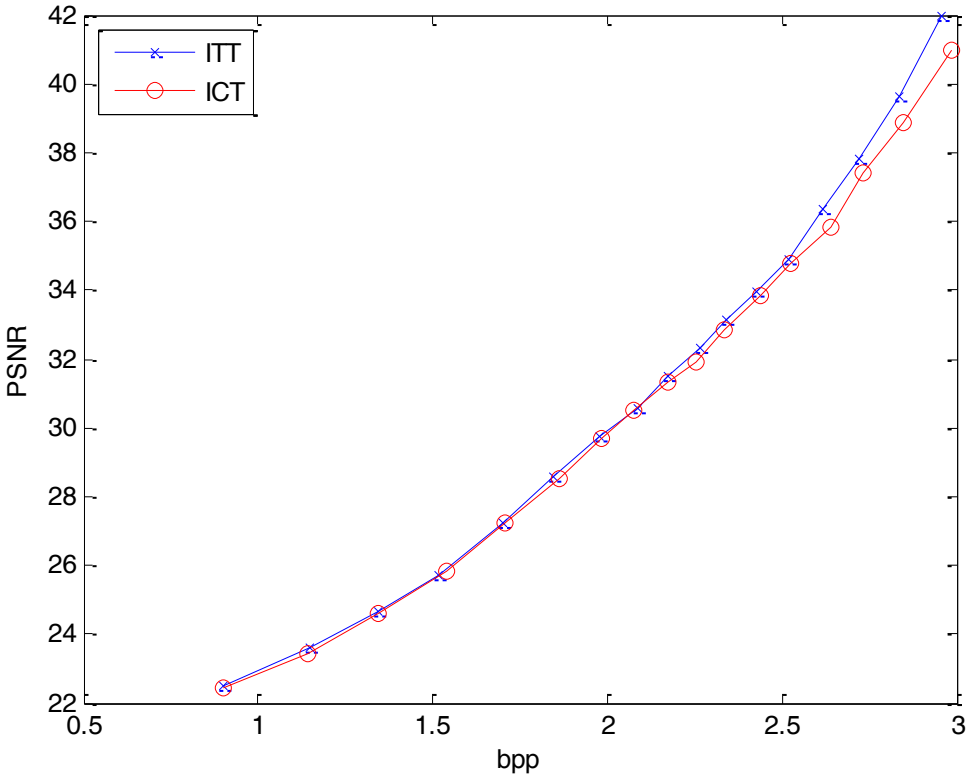

Figure 3.17: PSNR vs. bpp plot for 8X8 compression of the assorted patterns image

From Table 3.7 it can be observed that though the correlation-based measures and the HVS-based measures are close to their ideal values, they are not as close as they were for the more predictable images (Section 3.4.3) using either ITT or ICT. Similarly, the AD and MD values are also higher when compared to that with the previous inputs. This can be attributed to the lower predictability of the image. It can be observed from Fig. 3.16 that the RMSE plot of ITT is lower than that of ICT, whereas the PSNR plot is higher as seen from Fig. 3.17 indicating a better quality of compression. This indicates the superior performance of ITT-based compression in comparison with that of the ICT-based compression.

3.4.5 Intercede Image of Running Horses

The subsequent frames in a video are usually similar with very little variations. So it is prudent to transmit the difference between two frames instead of the entire frame data to drastically reduce the information to be transmitted. This practice is termed as interceding. Most of the current video compression techniques typically employ this technique but at the same time periodically transmit an entire frame data to ensure fidelity to the actual video. So it is interesting to note the results of compression on the subsequent frame difference image using ITT and ICT. The interceded image given in Fig. 3.18 is the difference between two concurrent frames of a video of horses running in a beach [27].

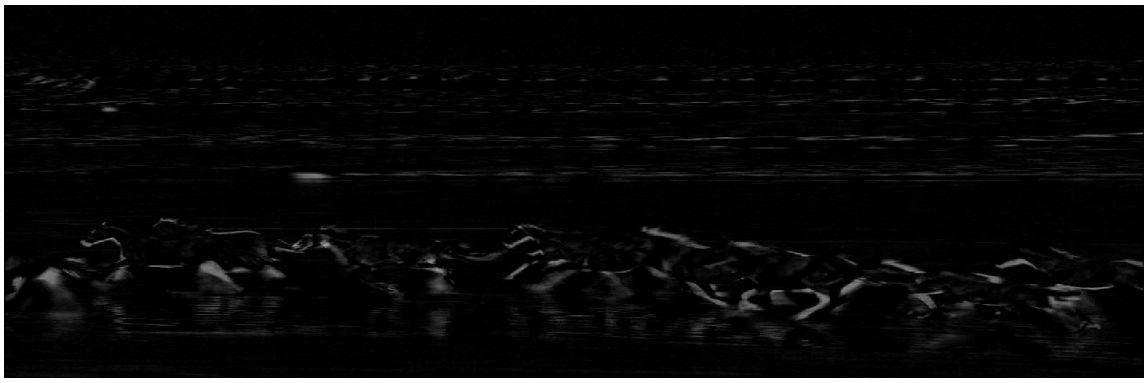

Figure 3.18: Intercede image of running horses video [27]

The size of the image is 1280×720 pixels and the SAM and SFM parameters are given by 65.0536 and 7.8822, respectively.

The RMSE and PSNR plots in Fig. 3.19 and Fig. 3.20 for ITT-and ICT-based compression of the intercede image are drawn based on the performance data given in Table 3.8.

Table 3.8: Quality Measures for 8X8 Image Compression of the intercede image of running horses video

Quality	5	10	15	30	35	40	45	60	65	80	85
ITT											
MSE	63.34	25.35	16.00	8.75	7.47	6.67	6.00	3.52	2.66	1.15	0.99
RMSE	7.96	5.03	4.00	2.96	2.73	2.58	2.45	1.88	1.63	1.07	1.00
PSNR	30.08	34.06	36.06	38.68	39.36	39.85	40.31	42.63	43.84	47.51	48.14
bpp	0.42	0.50	0.58	0.84	0.90	0.94	1.04	1.52	1.67	1.89	1.98
CR	19.18	16.01	13.77	9.49	8.92	8.49	7.73	5.27	4.78	4.23	4.03
NK	0.92	0.94	0.95	0.98	0.98	0.98	0.98	1.00	1.00	1.00	1.00
SC	0.86	0.99	1.02	1.00	1.00	1.00	1.00	0.98	0.98	1.00	1.00
NAE	1.22	0.57	0.46	0.34	0.32	0.30	0.29	0.20	0.18	0.11	0.10
LMSE	0.33	0.13	0.08	0.05	0.04	0.03	0.03	0.02	0.01	0.01	0.01
AD	6.75	3.17	2.53	1.87	1.76	1.68	1.60	1.11	0.99	0.59	0.55
MD	98.00	72.00	56.00	46.00	45.00	45.00	38.00	35.00	29.00	19.00	14.00
ICT											
MSE	69.80	26.90	17.78	9.44	8.10	7.61	7.49	3.69	2.57	1.13	1.19
RMSE	8.35	5.19	4.22	3.07	2.85	2.76	2.74	1.92	1.60	1.06	1.09
PSNR	29.66	33.80	35.60	38.35	39.01	39.28	39.35	42.42	43.99	47.56	47.34
bpp	0.42	0.50	0.58	0.87	0.89	0.90	0.98	1.68	1.79	1.85	1.87
CR	19.18	16.06	13.90	9.22	9.04	8.89	8.13	4.77	4.47	4.33	4.28
NK	0.93	0.95	0.96	1.00	0.99	0.99	0.99	1.03	1.03	1.01	1.02
SC	0.81	0.96	0.98	0.96	0.97	0.98	0.98	0.92	0.94	0.97	0.96
NAE	1.31	0.60	0.53	0.37	0.34	0.34	0.34	0.23	0.20	0.14	0.14
LMSE	0.36	0.14	0.09	0.05	0.04	0.04	0.04	0.02	0.01	0.01	0.01
AD	7.22	3.30	2.94	2.03	1.89	1.85	1.89	1.26	1.13	0.76	0.77
MD	95.00	64.00	59.00	37.00	38.00	37.00	35.00	22.00	18.00	8.00	10.00

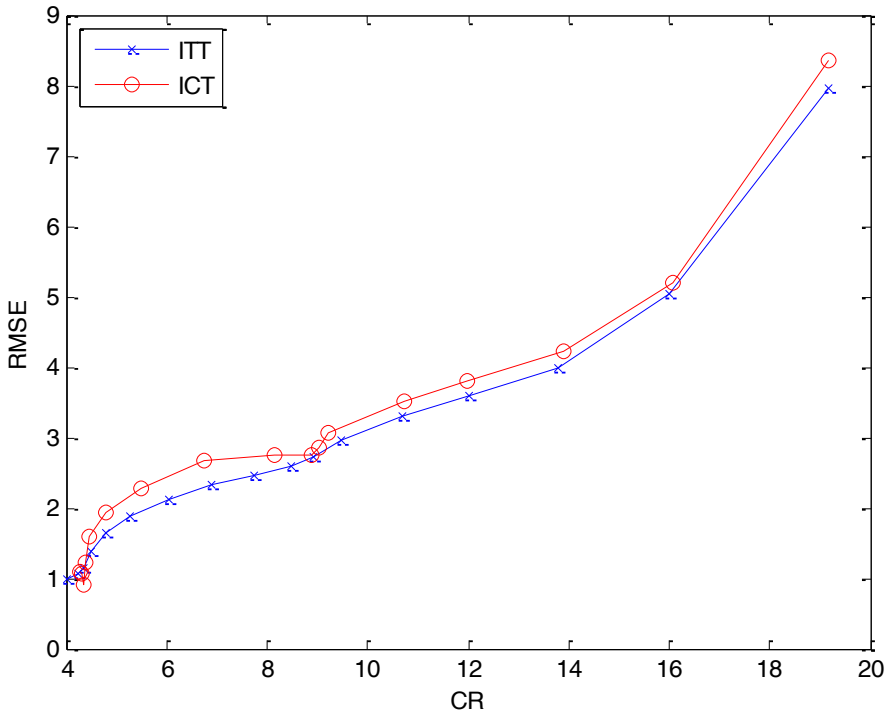

Figure 3.19: RMSE vs. CR plot for 8X8 compression of the intercede image of running horses video

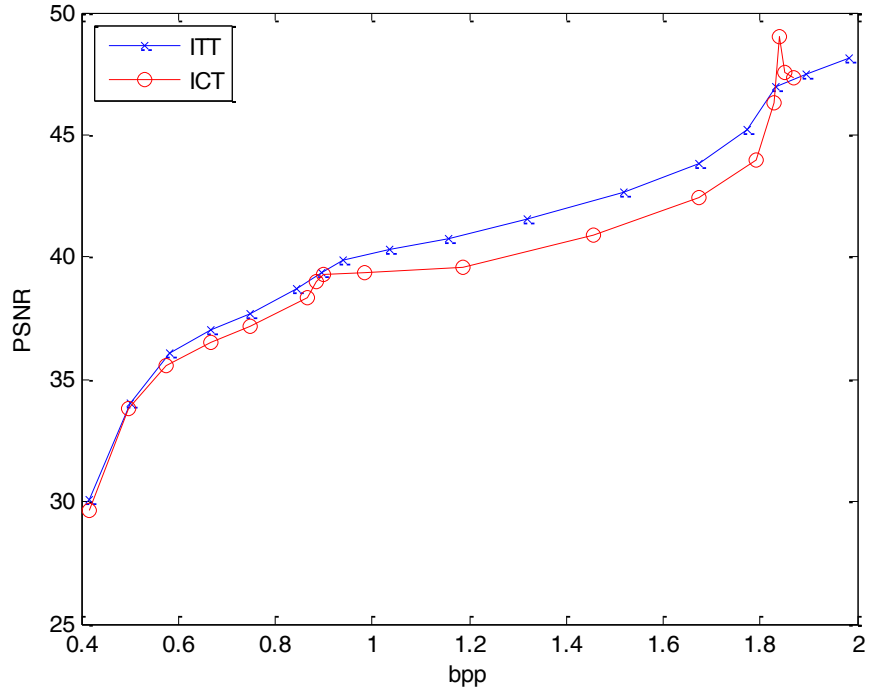

Figure 3.20: PSNR vs. bpp plot for 8X8 compression of the intercede image of running horses video

As the image has less predictability, the PQE parameters are slightly deviant from their ideal parameters at high rates of compression, similar to the scenario of Section 3.4.4. At any given CR, it can be observed from Fig. 3.19 that the RMSE of ITT is lower than that of ICT. Also, it can be noted that the PSNR curve of ITT is above that of ICT over a major range of bpp, as can be observed from Fig. 3.20. Hence, it is logical to deduce that ITT is a better choice over ICT for compression of the image.

3.4.6 Intercede Image of Flying Birds

Figure 3.21 depicts another intercede image which is from a video of flying birds [27]. The SAM and SFM parameters of the image are given as 47.97 and 6.72, respectively.

Figure 3.21: Intercede image of flying birds video [27]

Similar to the previous intercede image considered in Section 3.4.5, the image is subjected to compression using ITT and ICT and the evaluation parameters are calculated and tabulated in Table 3.9. Using this data, the performance plots in Fig. 3.22 and Fig. 3.23 are drawn to analyze the functioning of the compression techniques.

Table 3.9: Quality Measures for 8X8 Image Compression of the intercede image of flying birds video

Quality	5	10	15	30	35	40	45	60	65	80	85
ITT											
RMSE	8.36	4.22	3.85	2.74	2.56	2.54	2.31	1.80	1.57	1.05	0.98
PSNR	29.65	35.59	36.40	39.35	39.92	40.02	40.83	42.99	44.16	47.67	48.30
bpp	0.39	0.44	0.49	0.66	0.70	0.74	0.79	1.01	1.11	1.28	1.36
CR	20.34	18.20	16.26	12.12	11.37	10.86	10.14	7.90	7.19	6.23	5.90
NK	0.95	0.96	0.96	0.98	0.98	0.98	0.99	1.00	1.00	1.00	1.00
SC	0.84	1.01	1.01	1.01	1.01	1.00	1.00	0.99	0.99	1.00	1.00
NAE	1.63	0.38	0.55	0.24	0.22	0.32	0.20	0.15	0.13	0.08	0.08
LMSE	0.30	0.08	0.06	0.03	0.03	0.03	0.02	0.01	0.01	0.00	0.00
AD	7.55	1.76	2.54	1.09	1.04	1.50	0.93	0.68	0.61	0.37	0.35
MD	118	104	84	53	51	51	44	37	39	22	19
ICT											
RMSE	8.84	4.26	4.22	2.70	2.53	2.60	2.44	1.71	1.58	0.87	0.96
PSNR	29.17	35.50	35.59	39.47	40.02	39.79	40.33	43.46	44.10	49.34	48.47
bpp	0.39	0.44	0.49	0.68	0.70	0.71	0.75	1.10	1.18	1.23	1.24
CR	20.35	18.12	16.26	11.75	11.43	11.24	10.63	7.27	6.77	6.50	6.43
NK	0.96	0.97	0.98	1.00	0.99	0.99	0.99	1.02	1.02	1.01	1.01
SC	0.80	0.98	0.97	0.98	0.98	0.99	0.99	0.95	0.95	0.98	0.97
NAE	1.74	0.39	0.69	0.25	0.23	0.35	0.24	0.17	0.25	0.10	0.12
LMSE	0.33	0.08	0.08	0.03	0.03	0.03	0.03	0.01	0.01	0.00	0.00
AD	8.07	1.81	3.22	1.18	1.06	1.61	1.10	0.77	1.14	0.46	0.55
MD	132	83	77	58	54	51	44	32	22	12	15

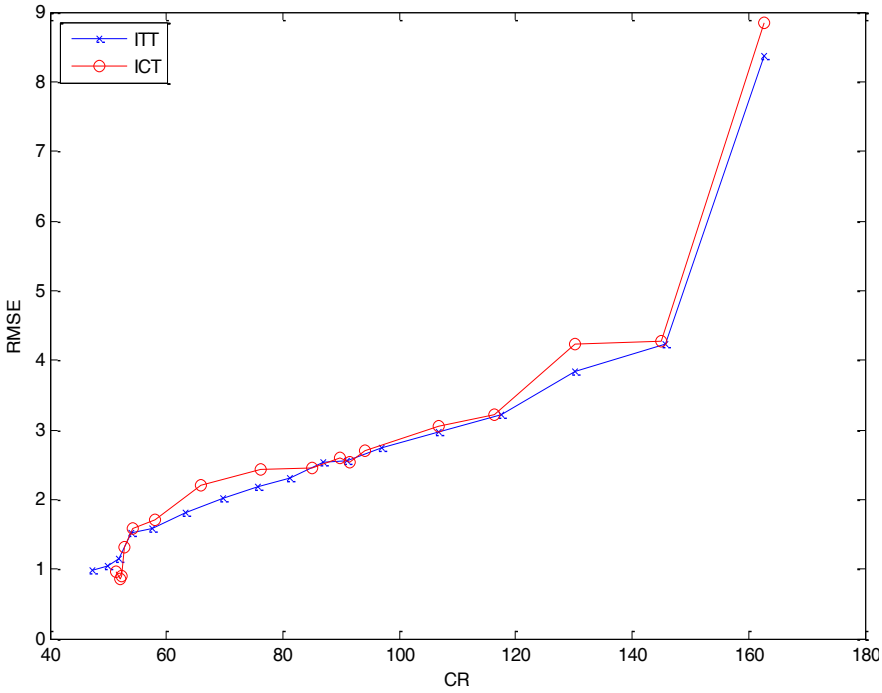

Figure 3.22: RMSE vs. CR plot for 8X8 compression of the intercede image of flying birds video

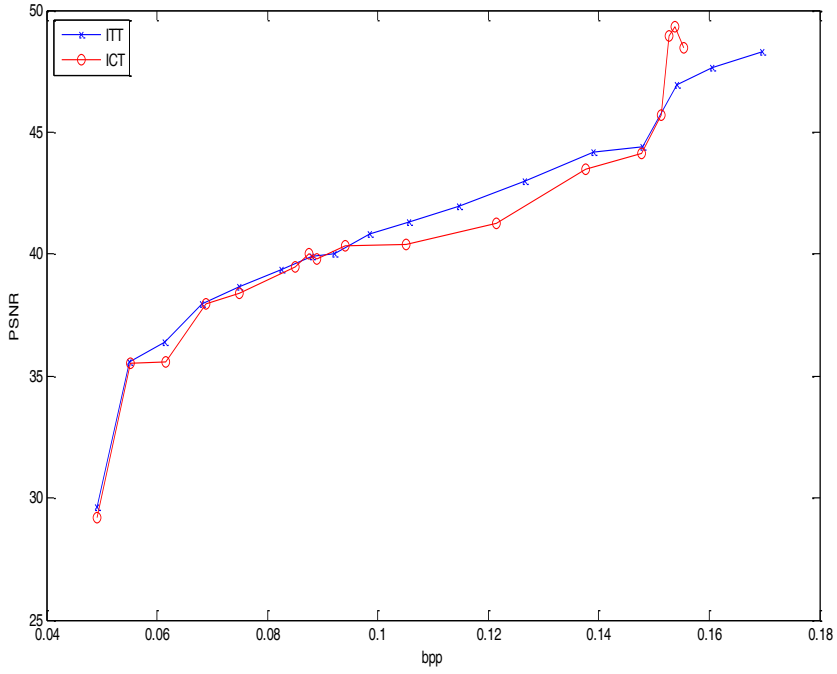

Figure 3.23: PSNR vs. bpp plot for 8X8 compression of the intercede image of flying birds video

It can be observed from the tabulated results in Table 3.9 and the plots in Fig. 3.22 and Fig. 3.23 that the performance is similar to that of the intercede image in the previous section. The ITT-based compression technique is found to offer a better PSNR and a lower RMSE than the ICT-based compression does. Based on the results in Section 3.4.5 and 3.4.6, it can be inferred that for compression of intercede images generated during video transmission; ITT-based technique provides a superior performance than that based on ICT.

From the above discussion of the compression results, it can be concluded that the performance of ITT is better than that of ICT for images that are less predictable with considerable spectral activity (assorted pattern and intercede images of Sections 3.4.4 - 3.4.6. The performance is almost the same in cases where SAM is moderate (Lena and Jupiter images of Sections 3.4.1 and 3.4.2), and slightly inferior for highly predictable images whose SAM is high (Cameraman image of Section 3.4.3). Thus, the efficiency of compression of an image depends not just on the compression technique adopted but also on the image characteristics themselves. In order to achieve optimal compression, it is beneficial to investigate and adopt a suitable compression technique based on the type of the input image.

3.5 Summary

In this Chapter, initially a multiplier-free fast implementation of the 8×8 ITT has been introduced. The arithmetic complexity of the proposed fast ITT was shown to be less than that of popular fast DCT and ICT implementations. In the subsequent section, the image compression performance of ITT and ICT have been evaluated and compared for diverse input images. The nature of images more suited for compression using ITT or ICT have been identified based on SFM and SAM characteristics of the images. Through simulations it has been shown that the

performance of ITT is about the same as ICT in most of the cases. It was also observed that although the compression performance of ITT can be slightly inferior to that of ICT for images with high predictability (SAM), it provides a better performance than ICT for images with low SAM.

The next chapter introduces a novel quantization technique to further enhance the compression of the images.

Chapter 4

Compression with variable quantization

4.1 Quantization

4.1.1 Need for Variable Quantization

A typical image has varying amount of detail spread across its area. It is unusual to encounter an image with homogenous distribution of data. Still a fixed quantization scheme which treats all the blocks of the image equally as discussed in Section 3.2.1 of the previous Chapter, is the norm in most of the lossy compression techniques. For instance, in JPEG format, once the level of compression desired is decided, the entire image is quantized with the same matrix. As a result all the blocks of the quantized output have the same accuracy level which might not always be the best choice.

An image is generally composed of a few blocks with high levels of detail which would be badly affected by quantization and the rest with lesser details which can withstand high levels of quantization. But the few susceptible blocks would be enough to bring down the quality of the image drastically. If the overall quantization factor is reduced in order to compensate for this loss of quality, then the compression efficiency diminishes. This substantiates the need for an alternative format, which adapts the quantization in accordance with the data contained by each block as described subsequently.

4.1.2 Variable Quantization:

For variable quantization, the blocks need to be differentiated as robust or sensitive to quantization based on their characteristics. Based on this classification, the quantization matrix to be employed during compression for each block is decided. The concept of variable quantization is illustrated in Fig. 4.1. The sensitive blocks are quantized with a smaller quantization matrix, whereas the resilient ones are quantized with a strong matrix. Thus the overall quality of the image is well maintained without having to sacrifice the compression rate.

One of the simplest ways of discriminating between the image blocks is based on their last non-zero element position (nzp) [28] after transformation followed by the standard quantization procedure described in Section 3.2.1. This position when compared with a threshold can help in determining if the block is strong enough to withstand high levels of quantization. It is possible to maintain multiple thresholds and quantize each image block that satisfies a threshold condition with the corresponding matrix. To decompress the image, each block needs to be de-quantized using the same matrix with which it was quantized. Hence, in [28] a predefined collection of quantization matrices were maintained at the transmitter and the receiver to avoid transmitting the entire quantization matrix along with each image block. However, this seriously hinders the flexibility of operation as the user is restricted to a pre-determined set of quantization matrices. For instance, the image block might be robust enough to withstand higher quantization, which might not be supported at the receiver. Depending on the type of images being compressed, the receiver might need to be updated periodically to ensure the adequacy of the quantization set. This predicament can be avoided by making the procedure truly adaptive and allowing the user a wider choice of quantization matrices without any additional transmission overhead.

The proposed method solves the problem stated above by employing a variable quantization factor instead of an entire matrix. If the nzp of the image block is less than the threshold, it is deemed to be robust and the elements of the already quantized block are quantized by an additional factor [29]. This factor is always chosen to be a multiple of '2', i.e., 2*p (p = 1,2,3..), such that the additional quantization i.e., division, can be accomplished by 'p' simple right shift operations. Consequently, the image block can be said to be quantized by '2p' times the standard quantized matrix given by (3.2).

If none of the threshold conditions are met then 'p' is set to '0' and no additional quantization is carried on the block. Thus, 'p = 0' indicates the corresponding image block to be sensitive to quantization.

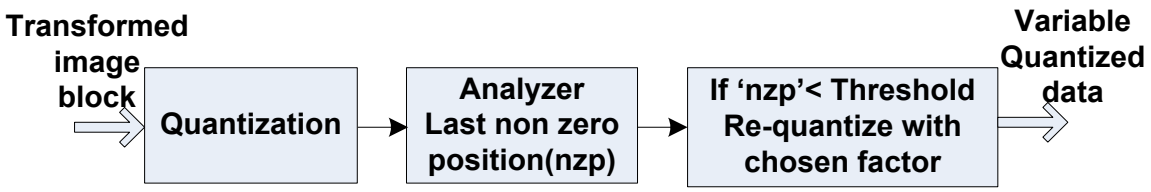

Figure 4.1: Variable Quantization scheme

For the current set of images chosen, the focus is to achieve high compression with least possible error. It has been found that the threshold value of '15' along with p =1, i.e., an additional quantization factor of '2', gives the best results in an 8×8 matrix. Hence, if the last non-zero element position of a transformed image block after being quantized with fixed quantization matrix is less than '15', then all the elements of the already quantized block undergo a single right shift to be additionally quantized by factor '2'. If the condition is not satisfied, there is no additional quantization. Thus, the blocks robust to quantization undergo double the quantization than the sensitive blocks.

As will be seen in Section 4.3, the variable quantized block is rearranged into a linear sequence and is subjected to encoding to further reduce its length. However, it must be noted that without the variable quantization information, the receiver cannot distinguish the blocks that underwent additional quantization from the normal blocks. Thus the variable quantization factor needs to be transmitted along with the compressed data to ensure faithful reconstruction. This can be achieved by the encoding technique described in Section 4.2.

4.2 Encoding

During decompression the image blocks must be de-quantized with the same matrix used for quantization, in order to reconstruct the original image. It would challenge the flexibility of the system if the actual set of quantization matrices is to be maintained at the transmitter as well as receiver. As, the matrix used for variable quantization is always a multiple of a fixed matrix, it would suffice to just transmit the quantization factor used for the block instead of the entire matrix. However, it needs to be coded into the compressed image information such that it would not lead to an increase in transmission data.

Conventional *run length encoding* (RLE) takes advantage of the fact that image data after transformation and quantization has significant number of zeros. RLE encodes by giving only the non-zero elements of the sequence. Each non-zero element (E) is preceded by the number of zeros (Z) before itself in the sequence. End of sequence is signified by setting both E and Z to zero. Fig. 4.2 illustrates an instance of conventional RLE carried on a data sequence.

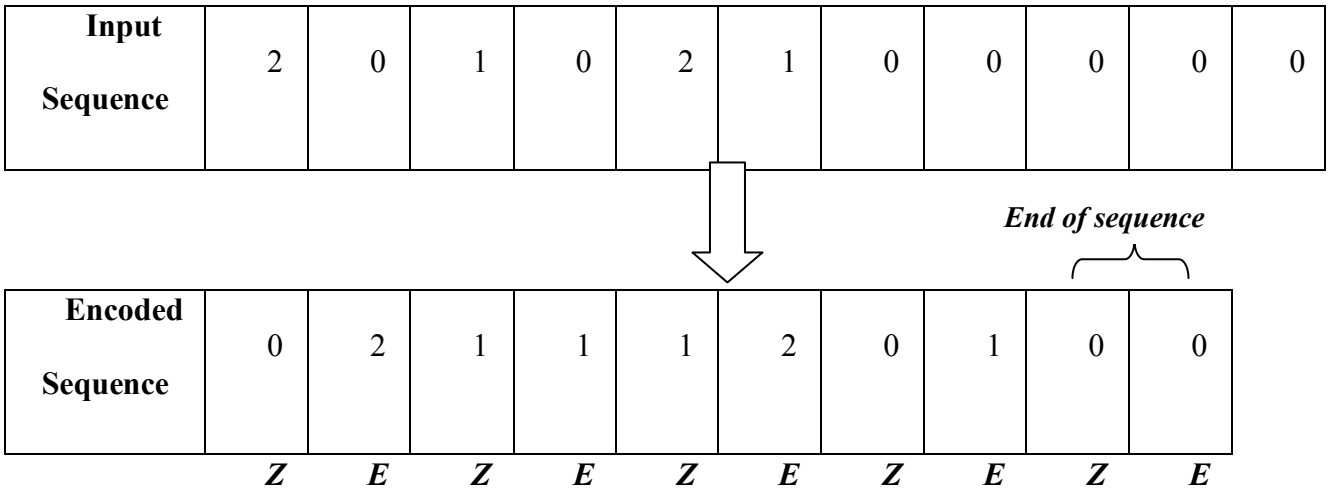

Figure 4.2: Conventional RLE Encoding

So it can be observed that in conventional RLE encoding, (E) can never be zero unless it is end of sequence.

In the modified RLE scheme (see Fig. 4.3), any additional bits to transmit quantization information can be avoided by making the last two codes (Z and E) at the end of block sequence, not only to indicate the end of the block but also its corresponding quantization factor. So at the end of the block sequence, E is set to zero indicating end of sequence and Z is set to ***`p`*** giving the variable quantization code.

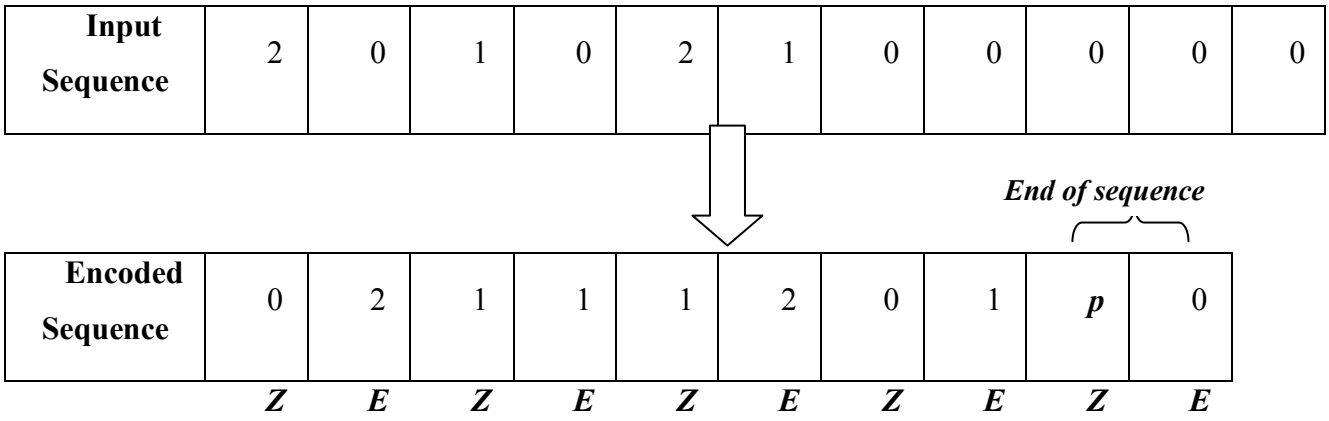

Figure 4.3: Modified RLE Encoding

At the decoder, the block is reconstructed and the variable quantization code `***p***` is identified as (Z) whose corresponding (E) is set to zero at the end of the sequence. The resulting block undergoes 'p' left shifts which is equivalent to being multiplied by `2*p` before being de-quantized with the fixed matrix as shown in Fig. 4.4.

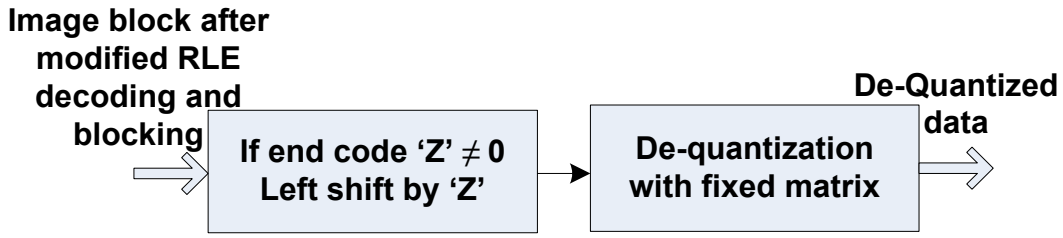

Figure 4.4: Variable de-quantization scheme

4.3 Compression and Decompression Schemes

The compression and decompression schemes to be followed for variable quantization are illustrated in Fig. 4.5 and Fig. 4.6, respectively. It can be perceived that the schemes are similar to those discussed in Section 3.2 except that variable quantization is used instead of standard quantization.

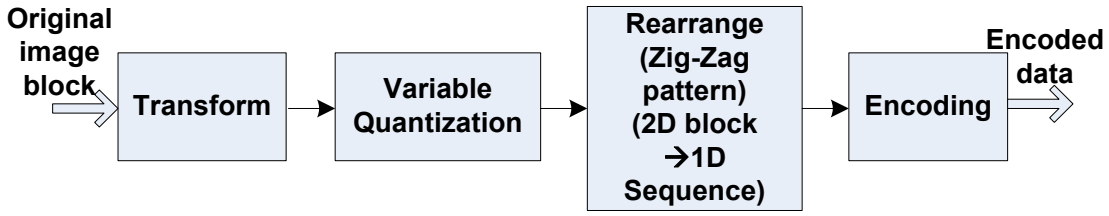

Figure 4.5: Variable Compression Scheme

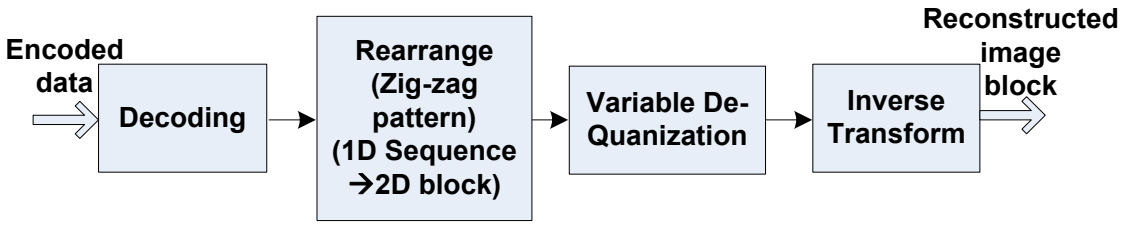

Figure 4.6: Variable decompression scheme

Table 4.1 gives a comparison of the arithmetic complexity of ICT [11] and ITT [14] with and without variable quantization.

Table 4.1: Comparison of Computational Complexity using variable Quantization

Input type	**Operation**	**ICT[11]**	**ITT[14]**	**ICT (variable quantization)**	**ITT (variable quantization)**
8 Point 1D array	Add	NA	44	NA	44
	Multiply	NA	0	NA	0
	Shift	NA	29	NA	29+ 8p[i]
8 Point 2D array	Add	448	704	448	704
	Multiply	352	0	352	0
	Shift	128	464	128+64p	464+64p

It can be observed that variable quantization preserves the virtue of multiplier-free implementation when used with ITT. It is seen that the variable quantization technique demands only an increase in the number of shift operations to compensate for the improved compression performance in case of ICT as well as ITT. The minor increase in the computational complexity due to the increase in the number of shift operations can be totally justified by the better compression performance obtained, as can be observed from the compression results of varied input images in Section 4.4.

[i] '2*p' is the additional quantization factor for the image block robust to quantization

4.4 Simulation

The variable image compression-decompression scheme described in Section 4.3 using both ITT and ICT is simulated with MATLAB [24] software. The compression quality results obtained for a variety of input images at different compression ratios using the method elucidated in Section 3.4 are analyzed. At the end of each simulation, the compression evaluation parameters listed in Section 3.3 are obtained. Using this data, the performance plots for each of the images are sketched following the procedure elucidated in Section 3.3.3.

Also, in order to compare the compression performance using variable quantization with that using fixed quantization discussed in Section 3.4, the performance curves for the latter and performance plots are redrawn for each image; this will facilitate us to decide if variable quantization is really worth the extra effort by yielding better results.

In these plots of PSNR vs. bpp and RMSE vs. CR the curves in black, green, red and blue indicate results for compression using ITT and ICT with and without variable quantization, respectively.

4.4.1 Lena Image

Compression with variable quantization using ITT and ICT is employed on the Lena image shown in Fig. 3.6. The image is of moderate predictability with considerable amount of frequency content, as mentioned in Section 3.6.1.

Compression with variable quantization using the chosen transform is carried out on the image at varying strengths of compression. At the end of each simulation, the resulting compression

evaluation parameter values are found and listed in Table 4.2. Table 3.4 carries the compression evaluation parameters of the same image with ITT-and ICT-based fixed quantization.

The performance curves of RMSE vs. CR as well as PSNR vs. bpp are plotted as Fig. 4.7 and Fig. 4.8, respectively, using the data in Table 4.2 and 3.4 for variable and fixed quantization, respectively.

Table 4.2: Quality Measures for 8X8 Image Compression of the Lena image with variable quantization

Quality	5	10	15	30	35	40	45	60	65	80	85
ITT (variable quantization)											
RMSE	13.60	9.72	7.86	5.54	5.16	4.89	4.61	4.04	3.83	3.08	2.74
PSNR	25.43	28.34	30.19	33.22	33.84	34.31	34.81	35.96	36.43	38.32	39.35
bpp	0.46	0.60	0.77	1.23	1.37	1.49	1.63	2.04	2.25	3.36	4.07
CR	17.49	13.29	10.35	6.50	5.84	5.37	4.91	3.93	3.56	2.38	1.96
NK	0.99	1.00	1.00	1.00	1.00	1.00	1.00	1.00	1.00	1.00	1.00
SC	1.00	1.00	1.00	1.00	1.00	1.00	1.00	1.00	1.00	1.00	1.00
NAE	0.08	0.05	0.04	0.03	0.03	0.03	0.03	0.02	0.02	0.02	0.02
LMSE	0.01	0.00	0.00	0.00	0.00	0.00	0.00	0.00	0.00	0.00	0.00
AD	9.72	6.89	5.64	4.08	3.81	3.62	3.42	3.00	2.84	2.27	2.02
MD	159	95	91	58	63	66	44	43	41	24	22
ICT (variable quantization)											
RMSE	13.57	9.66	7.79	5.46	5.08	4.81	4.54	3.98	3.75	3.05	2.73
PSNR	25.45	28.40	30.26	33.36	33.99	34.46	34.95	36.11	36.61	38.42	39.37
bpp	0.46	0.60	0.76	1.21	1.35	1.48	1.62	2.03	2.26	3.36	4.08
CR	17.47	13.37	10.54	6.61	5.91	5.41	4.94	3.93	3.54	2.38	1.96
NK	1.00	1.00	1.00	1.00	1.00	1.00	1.00	1.00	1.00	1.00	1.00
SC	0.99	1.00	0.99	0.99	0.99	0.99	0.99	0.99	0.99	0.99	0.99
NAE	0.08	0.05	0.04	0.03	0.03	0.03	0.03	0.02	0.02	0.02	0.02
LMSE	0.01	0.00	0.00	0.00	0.00	0.00	0.00	0.00	0.00	0.00	0.00
AD	9.73	6.89	5.64	4.07	3.79	3.61	3.41	2.99	2.82	2.28	2.04
MD	180	94	77	50	53	56	54	46	37	33	19

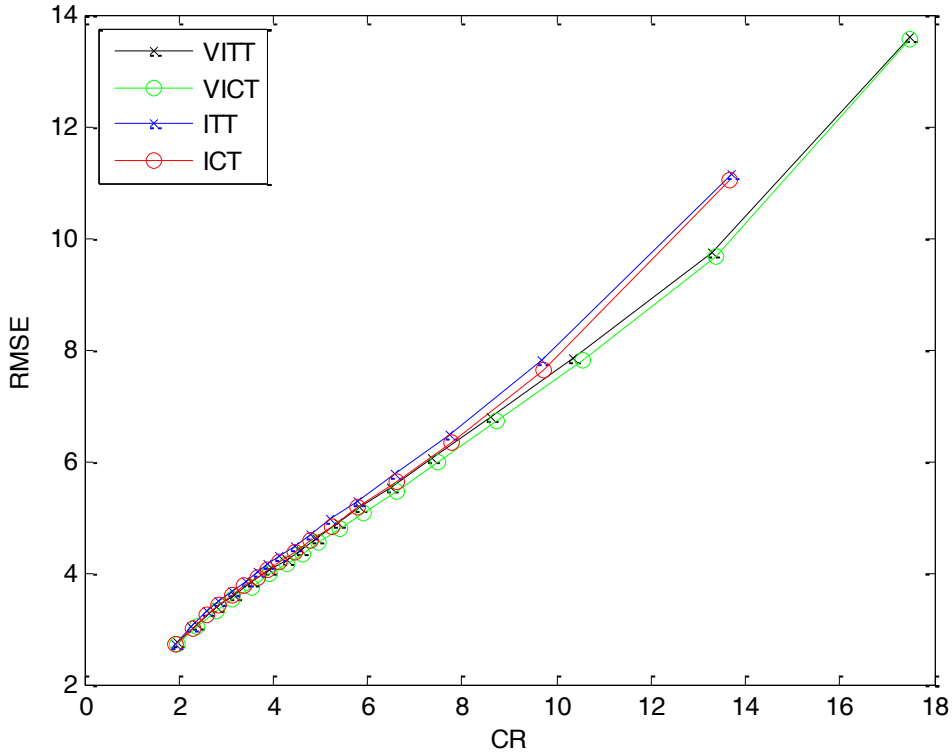

Figure 4.7: RMSE vs. CR plot for 8X8 compression of the Lena image

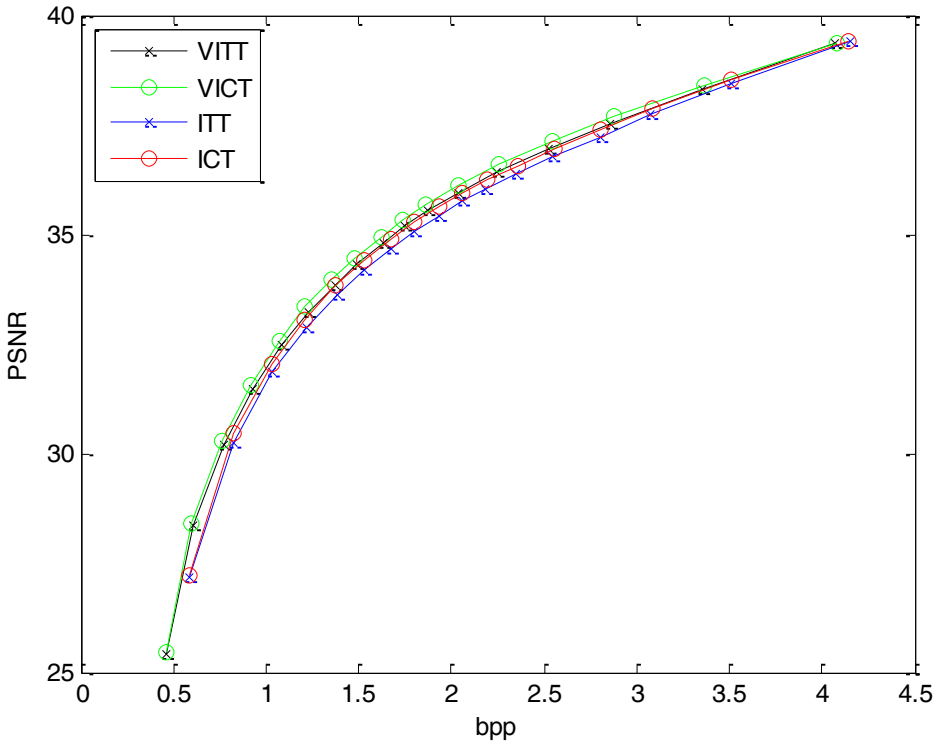

Figure 4.8: PSNR vs. bpp plot for 8X8 compression of the Lena image

By comparing the data in Tables 4.2 and Table 3.4 it may be observed that at any given `*Quality*` factor the quality evaluation parameters for non-variable compression are slightly better than those of variable compression. However, it can also be noted that the compression evaluation parameters namely CR and bpp are better for variable quantization. The rest of the quality evaluation measures discussed in Section 3.3.1 are not too deviant from their ideal values except for MD. There is an increase in MD when images are compressed with variable quantization as can be observed from Tables 4.2 and 3.4. However, this can be ignored since an increase in MD does not necessarily mean overall poor quality of the image. In order to make a prudent choice between variable and non-variable approaches, the performance must be compared at the same level of compression for both of them. This can be accomplished by studying the corresponding performance plots of the image compression. From the RMSE vs. CR plot in Fig. 4.7 it can be observed that RMSE curve for compression using variable quantization is significantly lower than that with normal quantization. Similarly, from the plot in Fig. 4.8 it is observed that the PSNR is higher at higher compression levels with variable quantization using either ITT or ICT than that with normal quantization. The PSNR and RMSE plots of ITT are almost overlapping with those of ICT in both the variable and non variable quantization cases. From this analysis, it can be inferred that compression using variable quantization is beneficial for images with moderate predictability and considerable frequency content.

4.4.2 Cameraman Image

Fig. 3.12 depicts the cameraman image of high predictability and frequency content similar to the Lena image considered in Section 4.4.1. On such an image, compression using ITT and ICT with variable quantization for various levels of compression is carried out and the results are

tabulated in Table 4.3. The corresponding results for the case without variable quantization are already given in Table 3.6.

Figs. 4.9 and 4.10 depict the RMSE vs. bpp and PSNR vs. CR plots obtained using the data in Tables 4.3 and 3.6.

Table 4.3: Quality Measures for 8X8 Image Compression of the Cameraman image with variable quantization

Quality	5	10	15	30	35	40	45	60	65	80	85
ITT (variable quantization)											
RMSE	12.84	8.90	6.96	4.54	4.13	3.85	3.58	3.01	2.79	2.10	1.78
PSNR	25.93	29.11	31.24	34.95	35.77	36.39	37.02	38.53	39.18	41.67	43.08
bpp	0.45	0.58	0.73	1.13	1.24	1.34	1.44	1.71	1.84	2.47	2.97
CR	17.70	13.68	11.02	7.06	6.43	5.98	5.55	4.68	4.34	3.24	2.70
NK	1.00	1.00	1.00	1.00	1.00	1.00	1.00	1.00	1.00	1.00	1.00
SC	1.00	1.00	1.00	1.00	1.00	1.00	1.00	1.00	1.00	1.00	1.00
NAE	0.07	0.05	0.04	0.03	0.02	0.02	0.02	0.02	0.02	0.01	0.01
LMSE	0.01	0.00	0.00	0.00	0.00	0.00	0.00	0.00	0.00	0.00	0.00
AD	8.60	5.90	4.52	3.06	2.81	2.64	2.47	2.10	1.95	1.48	1.25
MD	148	106	78	46	38	39	32	33	25	23	18
ICT(variable quantization)											
RMSE	12.74	8.85	6.87	4.41	3.99	3.70	3.44	2.91	2.71	2.07	1.81
PSNR	25.99	29.16	31.36	35.21	36.08	36.74	37.37	38.83	39.44	41.78	42.95
bpp	0.45	0.57	0.71	1.11	1.23	1.32	1.42	1.68	1.81	2.42	2.90
CR	17.76	13.93	11.21	7.19	6.51	6.06	5.65	4.77	4.43	3.31	2.76
NK	1.00	1.00	1.00	1.00	1.00	1.00	1.00	1.00	1.00	1.00	1.00
SC	0.99	0.99	0.99	0.99	0.99	0.99	0.99	0.99	0.99	0.99	0.99
NAE	0.07	0.05	0.04	0.03	0.02	0.02	0.02	0.02	0.02	0.01	0.01
LMSE	0.01	0.00	0.00	0.00	0.00	0.00	0.00	0.00	0.00	0.00	0.00
AD	8.55	5.92	4.56	3.05	2.80	2.62	2.45	2.11	1.97	1.53	1.34
MD	147	98	87	49	43	37	30	32	27	22	14

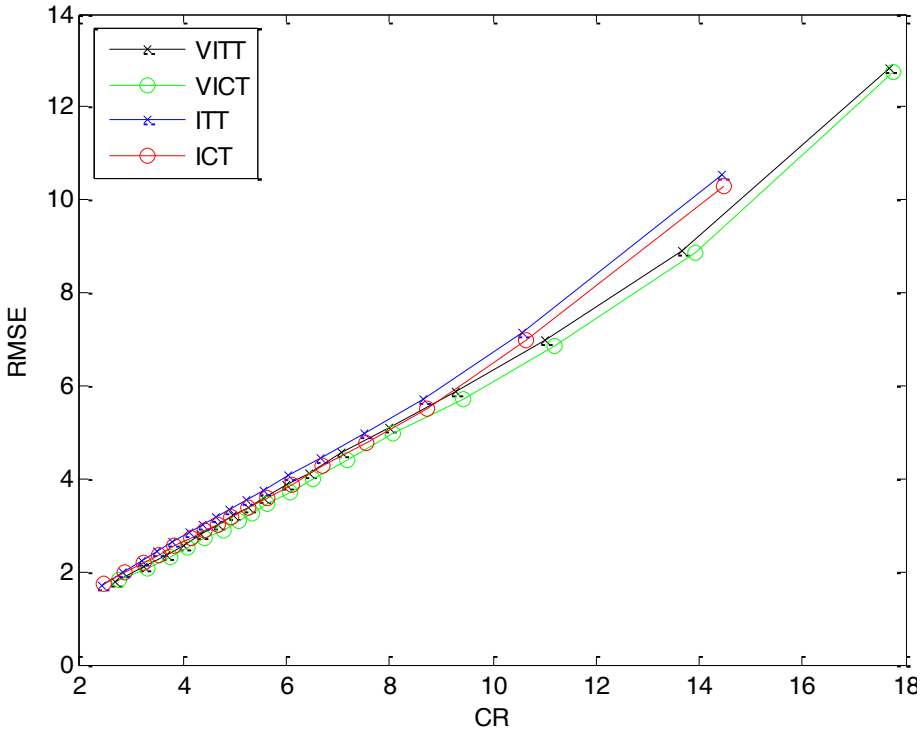

Figure 4.9: RMSE vs. CR plot for 8X8 compression of the Cameraman image

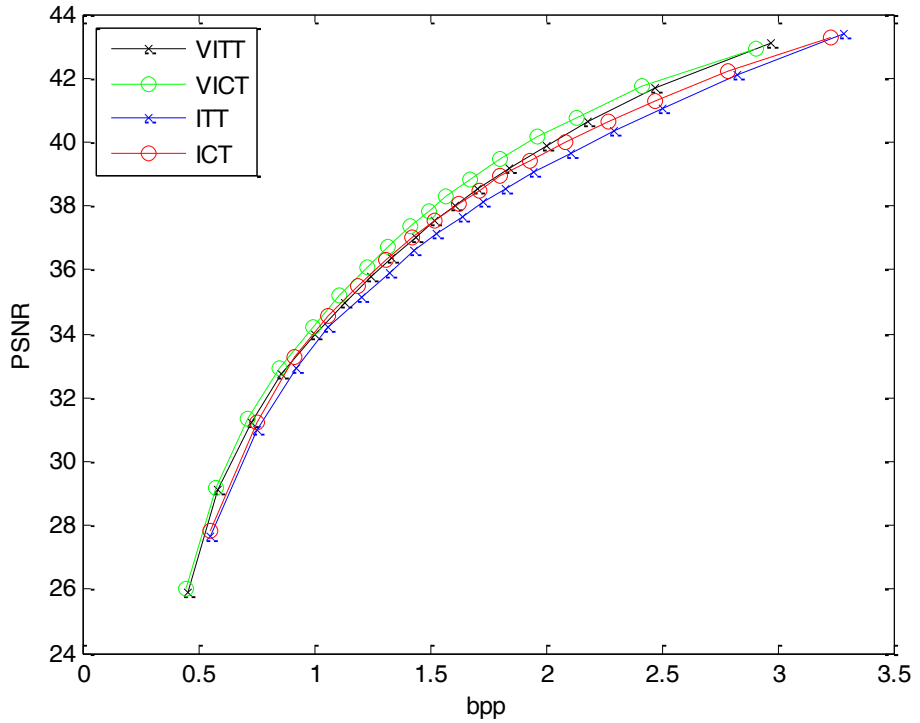

Figure 4.10: PSNR vs. bpp plot for 8X8 compression of the Cameraman image

From the Table 4.3, it can be observed that the results obtained for this image are similar to those obtained for the Lena image in Section 4.4.1. It can be noticed from the plots in Fig. 4.9 and Fig. 4.10 that compression with variable quantization offers better results than that with fixed quantization using either ITT or ICT as its corresponding PSNR vs. bpp curve is higher and RMSE vs. CR curve is lower than that with standard quantization. It can also be stated that variable quantization offers a wider range of compression, without much deterioration in quality than that offered by standard quantization, as can be observed from the RMSE vs. CR plot in Fig 4.9. Thus, it can be asserted that a better compression performance can be attained by using variable quantization for images with considerable frequency content.

4.4.3 Assorted Patterns Image

The image shown in Fig. 3.15 and described in Section 3.4.4 is an assorted collection of patterns. It has a high SFM of 63.6 indicating high frequency content compared to the images previously considered in Sections 4.4.1 and 4.4.2.

The image is subjected to variable quantization based compression using ITT transform. The reconstructed image is compared with the uncompressed image and the quality of the final image is evaluated. The process is iterated for varying levels of compression as discussed initially in Section 4.4. The entire procedure is repeated by using ICT instead of ITT and the outcomes are recorded. The various quality parameters of the compression performance using variable quantized ITT and variable quantized ICT are consolidated in Table 4.4. The various quality parameters of the compression performance using ITT and ICT with normal quantization have already been listed in Table 3.7. The RMSE and PSNR plots in Fig. 4.11 and Fig. 4.12 are drawn based on the data and results in Tables 3.7 and 4.4.

Table 4.4: Quality Measures for 8X8 Image Compression of the assorted patterns image with variable quantization

Quality	5	10	15	30	35	40	45	60	65	80	85
ITT(variable quantization)											
RMSE	19.82	16.89	14.91	9.45	8.28	7.54	6.76	5.08	4.57	2.64	2.03
PSNR	22.16	23.54	24.63	28.58	29.74	30.55	31.50	33.97	34.90	39.65	41.96
bpp	0.85	1.13	1.34	1.84	1.97	2.08	2.17	2.42	2.52	2.83	2.96
CR	9.37	7.10	5.99	4.35	4.05	3.84	3.68	3.30	3.18	2.82	2.71
NK	0.98	0.99	0.98	0.99	0.99	0.99	1.00	1.00	0.99	1.00	1.00
SC	1.03	1.02	1.03	1.01	1.01	1.02	1.01	1.00	1.01	1.00	1.00
NAE	0.03	0.03	0.03	0.01	0.01	0.01	0.01	0.01	0.01	0.00	0.00
LMSE	0.01	0.01	0.00	0.00	0.00	0.00	0.00	0.00	0.00	0.00	0.00
AD	6.69	5.62	5.51	2.75	2.40	2.97	1.99	1.53	2.04	0.80	0.61
MD	255	248	254	169	143	113	104	69	60	37	28
ICT(variable quantization)											
RMSE	19.94	17.25	15.01	9.55	8.35	7.57	6.91	5.18	4.64	2.89	2.27
PSNR	22.10	23.36	24.57	28.49	29.66	30.51	31.30	33.82	34.76	38.87	40.96
bpp	0.85	1.12	1.34	1.85	1.98	2.07	2.17	2.43	2.52	2.85	2.98
CR	9.37	7.17	5.99	4.31	4.05	3.86	3.69	3.29	3.17	2.81	2.68
NK	0.99	0.99	0.99	1.00	1.00	0.99	1.00	1.00	1.00	1.00	1.00
SC	1.02	1.02	1.02	1.00	1.01	1.01	1.00	1.00	1.00	1.00	0.99
NAE	0.03	0.03	0.03	0.02	0.01	0.01	0.01	0.01	0.01	0.01	0.01
LMSE	0.01	0.01	0.00	0.00	0.00	0.00	0.00	0.00	0.00	0.00	0.00
AD	6.28	5.52	5.13	3.52	2.55	2.56	2.75	1.70	1.56	1.55	1.34
MD	249	249	246	161	129	138	116	71	69	34	25

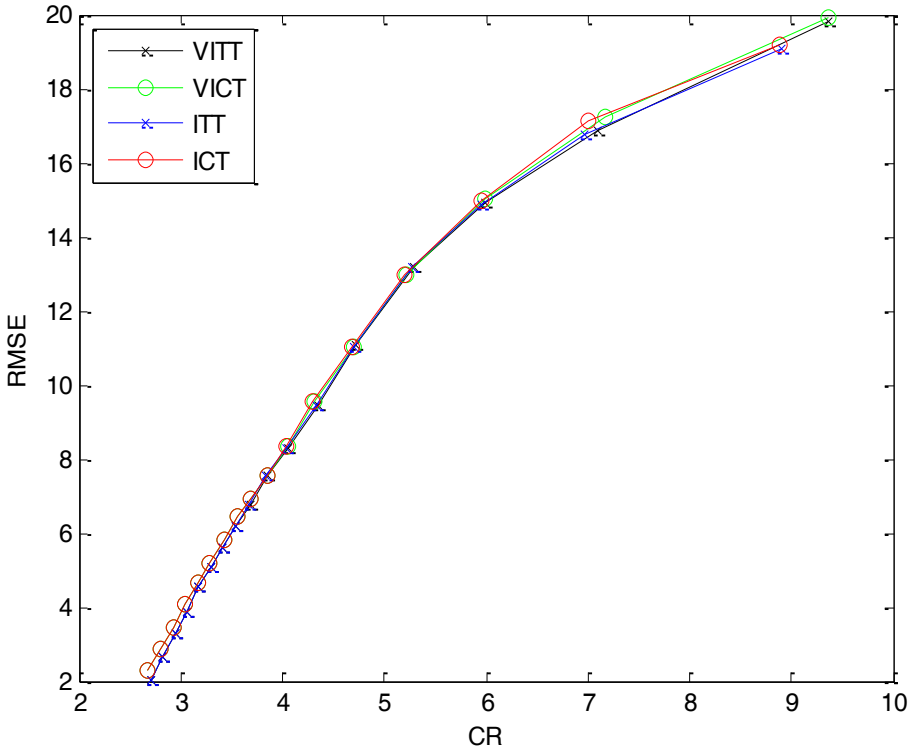

Figure 4.11: RMSE vs. CR plot for 8X8 compression of the assorted patterns image

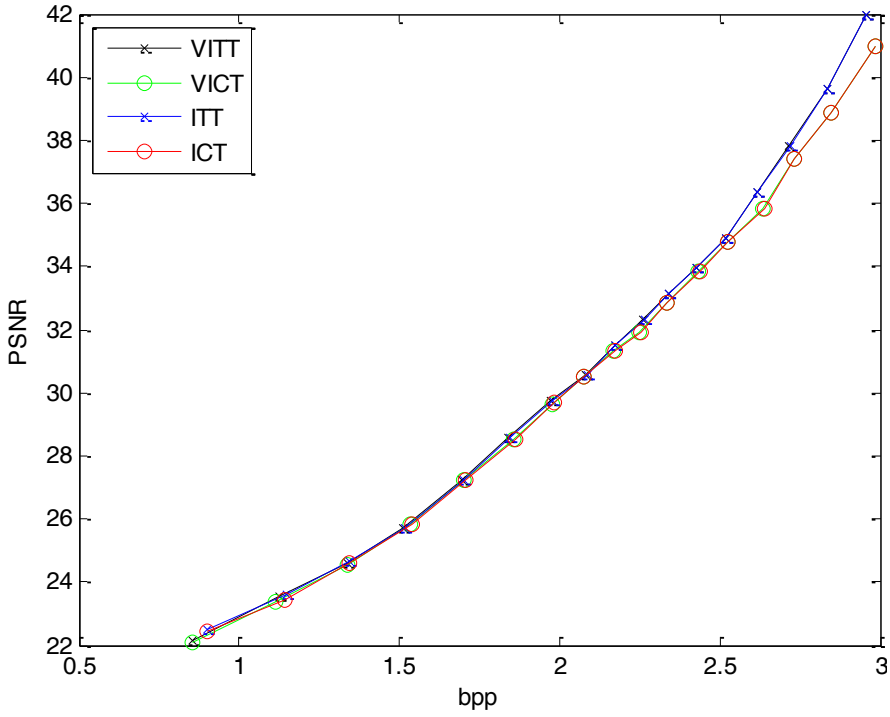

Figure 4.12: PSNR vs. bpp plot for 8X8 compression of the assorted patterns image

It can be observed from the performance plots in Fig. 4.11 and Fig. 4.12 that the RMSE plot of ITT is lower than that of ICT, whereas the PSNR plot is higher. This indicates the superior performance of ITT-based compression in comparison with that of the ICT-based one. The plots also indicate that compression using variable quantization is very similar to that obtained using normal quantization as the curves for variable and non variable quantization based compression overlap for ITT as well as ICT. This can be attributed to the high SFM value of the image, which indicates the presence of intricate detail. So abiding by the law of variable quantization, the majority of blocks cannot withstand high levels of quantization and so undergo usual quantization. This similarity in performance is also noticed by comparing the data in Tables 3.7 and 4.4 where almost all the parameters follow similar pattern. Thus, it can be stated that variable quantization and standard quantization based compression techniques yield similar results for images with high SFM.

4.4.4 Intercede Image of Running Horses

Variable quantized compression is carried out on the intercede image shown in Fig. 3.18. The image has very low spectral activity as indicated by the low SFM value of 7.8822.

Abiding by the practice followed for the image compression carried out in the previous sections, (4.4.1 - 4.4.3), the results of compression of the interceded image using variable quantization are captured in Table 4.5. Table 3.8 lists results obtained by following a similar procedure but of compression using standard quantization of the image. The RMSE vs. CR and PSNR vs. bpp plots of the ITT-and ICT-based variable and fixed compression of the intercede image are drawn in Fig. 4.13 and Fig. 4.14, respectively, based on the performance data in Tables 4.5 and 3.8.

Table 4.5: Quality Measures for 8X8 Image Compression of the intercede of running horses video with variable quantization

Quality	5	10	15	30	35	40	45	60	65	80	85
ITT(variable quantization)											
RMSE	8.91	5.97	4.83	3.40	3.11	2.90	2.73	2.12	1.90	1.22	1.02
PSNR	29.10	32.57	34.41	37.48	38.25	38.84	39.37	41.56	42.51	46.37	47.95
bpp	0.39	0.42	0.48	0.67	0.73	0.78	0.84	1.16	1.29	1.77	1.95
CR	20.77	18.93	16.76	12.03	10.92	10.25	9.49	6.89	6.20	4.52	4.09
NK	0.83	0.90	0.92	0.97	0.97	0.98	0.98	0.99	1.00	1.00	1.00
SC	0.92	1.02	1.03	1.01	1.00	1.00	1.00	0.99	0.99	1.00	1.00
NAE	1.30	0.66	0.53	0.39	0.37	0.35	0.33	0.25	0.24	0.14	0.10
LMSE	0.41	0.19	0.12	0.06	0.05	0.04	0.04	0.02	0.02	0.01	0.01
AD	7.15	3.62	2.92	2.17	2.03	1.91	1.82	1.37	1.30	0.75	0.57
MD	119	96	79	55	45	45	38	35	29	19	14
ICT(variable quantization)											
RMSE	9.27	6.13	5.03	3.52	3.26	3.11	3.04	2.11	1.82	1.24	1.11
PSNR	28.75	32.35	34.07	37.18	37.84	38.24	38.43	41.61	42.89	46.21	47.16
bpp	0.39	0.42	0.47	0.68	0.72	0.74	0.78	1.34	1.42	1.77	1.85
CR	20.77	18.99	16.92	11.83	11.09	10.74	10.21	5.98	5.62	4.53	4.31
NK	0.85	0.91	0.94	0.99	0.99	0.99	0.99	1.03	1.02	1.01	1.02
SC	0.87	0.99	0.99	0.97	0.97	0.98	0.98	0.93	0.94	0.96	0.96
NAE	1.38	0.68	0.60	0.43	0.39	0.38	0.39	0.27	0.24	0.16	0.14
LMSE	0.45	0.19	0.13	0.06	0.06	0.05	0.05	0.02	0.02	0.01	0.01
AD	7.62	3.76	3.33	2.35	2.18	2.10	2.13	1.47	1.35	0.88	0.79
MD	113	95	101	42	38	40	35	22	18	9	10

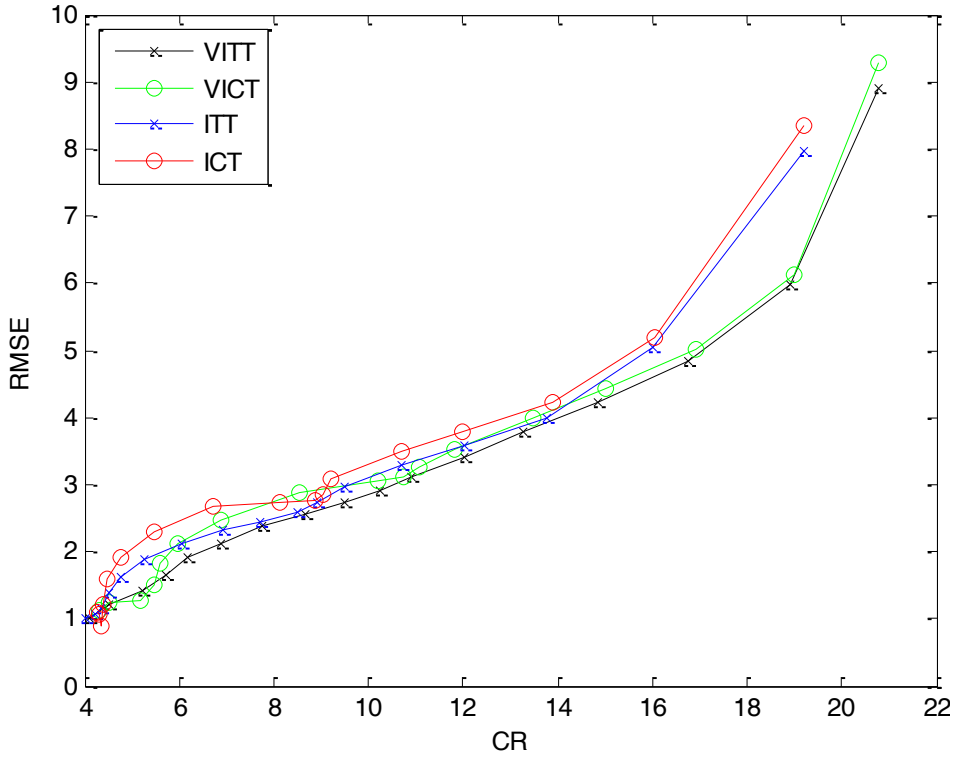

Figure 4.13: RMSE vs. CR plot for 8X8 compression of the intercede image of running horses

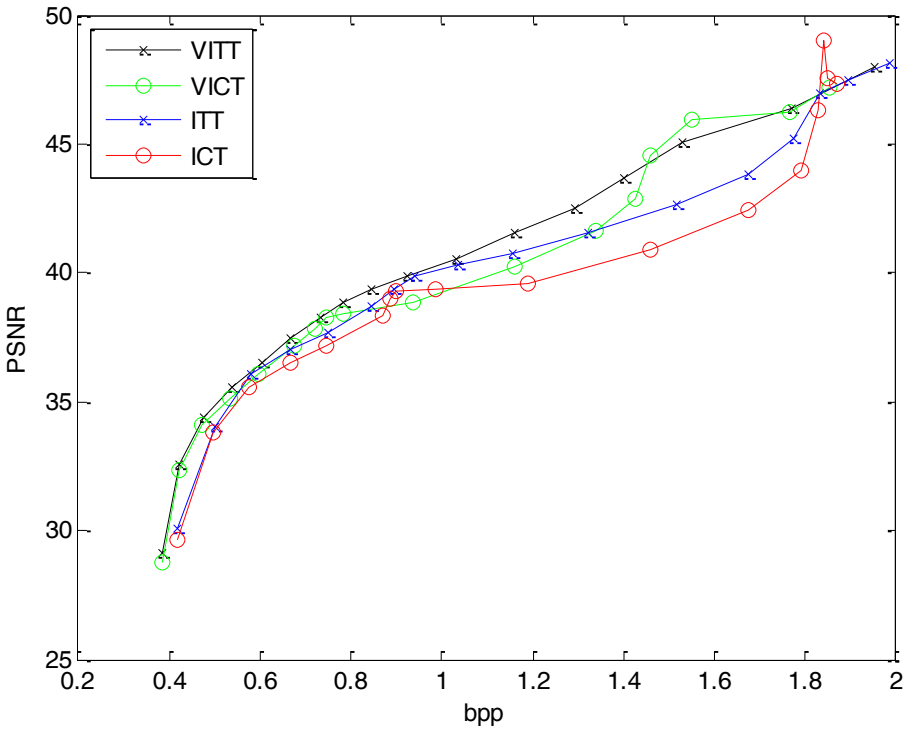

Figure 4.14: PSNR vs. bpp plot for 8X8 compression of the intercede image of running horses

From the RMSE vs. CR plot in Fig. 4.13 it can be seen that compression with variable quantization offers better quality than that offered with standard quantization on account of its low RMSE even at high CR irrespective of the transform used. Moreover, PSNR of the proposed compression method is consistently better than that with the conventional method, as can be noticed in the plot in Fig. 4.14. Based on these observations, it can be inferred that variable ITT offers the best compression result followed by variable ICT, ITT and ICT at higher compression ratios for the intercede image.

4.4.5 Hand-written Letter Image

Fig. 4.15 depicts a handwritten message by the poet Rabindranath Tagore to an acquaintance. The SAM and SFM parameters of the image are given as 664.7 and 26.2, respectively. The effect of variable quantization on hand written scripts is interesting to observe as they often need to be scanned as images before being stored or transmitted. So there is a quest to find ways to compress such images effectively without much deterioration in quality.

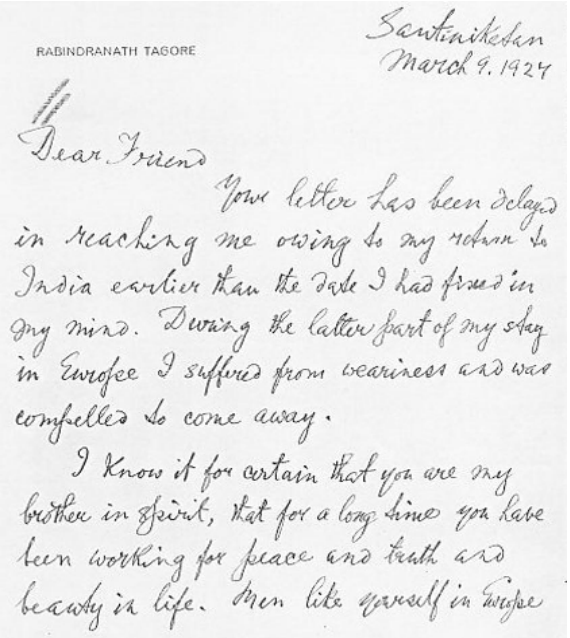
RABINDRANATH TAGORE

Santiniketan
March 9. 1924

Dear Friend

Your letter has been delayed in reaching me owing to my return to India earlier than the date I had fixed in my mind. During the latter part of my stay in Europe I suffered from weariness and was compelled to come away.

I know it for certain that you are my brother in spirit, that for a long time you have been working for peace and truth and beauty in life. Men like yourself in Europe

Figure 4.15: Hand-written letter [30]

The image in Fig. 4.15 is compressed using ITT-and ICT-based compression techniques with and without variable quantization. The simulations are carried out for a wide range of compression levels and the corresponding evaluation parameters are recorded in Table 4.6 and Table 4.7 for compression with standard quantization and variable quantization, respectively. The corresponding performance plots are depicted in Fig. 4.16 and Fig. 4.17.

Table 4.6: Quality Measures for 8X8 Image Compression of the scanned Hand-written letter

Quality	5	10	15	30	35	40	45	60	65	80	85
ITT											
RMSE	12.66	9.24	7.49	5.34	4.91	4.59	4.31	3.51	3.23	2.32	1.95
PSNR	26.05	28.78	30.60	33.55	34.28	34.86	35.41	37.18	37.92	40.78	42.31
bpp	0.72	0.97	1.14	1.53	1.62	1.69	1.83	2.39	2.50	2.84	3.04
CR	11.09	8.25	7.03	5.23	4.95	4.74	4.37	3.35	3.20	2.82	2.63
NK	1.01	1.00	1.00	1.00	1.00	1.00	1.00	1.00	1.00	1.00	1.00
SC	0.99	1.00	1.00	1.00	1.00	1.00	1.00	1.00	1.00	1.00	1.00
NAE	0.03	0.02	0.02	0.01	0.01	0.01	0.01	0.01	0.01	0.01	0.00
LMSE	0.00	0.00	0.00	0.00	0.00	0.00	0.00	0.00	0.00	0.00	0.00
AD	7.16	5.66	4.31	3.03	2.81	2.66	2.50	1.93	1.70	1.19	1.02
MD	151	109	87	68	62	55	50	40	42	26	25
ICT											
RMSE	12.08	8.67	6.97	4.71	4.34	4.17	4.11	2.61	2.12	1.39	1.26
PSNR	26.45	29.34	31.23	34.63	35.34	35.69	35.83	39.76	41.58	45.23	46.11
bpp	0.72	0.96	1.09	1.54	1.55	1.55	1.67	2.59	2.61	2.62	2.62
CR	11.05	8.35	7.31	5.18	5.17	5.15	4.78	3.09	3.06	3.05	3.05
NK	1.01	1.01	1.00	1.00	1.00	1.00	1.00	1.00	1.00	1.00	1.00
SC	0.98	0.99	0.99	1.00	1.00	1.00	1.00	1.00	1.00	1.00	1.00
NAE	0.03	0.02	0.02	0.01	0.01	0.01	0.01	0.01	0.01	0.00	0.00
LMSE	0.00	0.00	0.00	0.00	0.00	0.00	0.00	0.00	0.00	0.00	0.00
AD	7.28	5.68	4.45	2.90	2.62	2.54	2.51	1.62	1.34	0.94	0.86
MD	236	98	81	60	60	46	48	34	36	15	12

Table 4.7: Quality Measures for 8X8 Image Compression of the scanned Hand-written letter with variable quantization

Quality	5	10	15	30	35	40	45	60	65	80	85
ITT(variable quantization)											
RMSE	15.87	10.02	7.78	5.45	5.01	4.68	4.39	3.59	3.32	2.37	1.95
PSNR	24.08	28.08	30.27	33.37	34.11	34.69	35.25	36.99	37.66	40.59	42.28
bpp	0.58	0.89	1.08	1.43	1.53	1.60	1.69	2.13	2.23	2.81	3.04
CR	13.81	9.02	7.41	5.57	5.22	4.99	4.72	3.75	3.59	2.84	2.63
NK	1.00	1.00	1.00	1.00	1.00	1.00	1.00	1.00	1.00	1.00	1.00
SC	0.99	1.00	1.00	1.00	1.00	1.00	1.00	1.00	1.00	1.00	1.00
NAE	0.04	0.03	0.02	0.01	0.01	0.01	0.01	0.01	0.01	0.01	0.00
LMSE	0.00	0.00	0.00	0.00	0.00	0.00	0.00	0.00	0.00	0.00	0.00
AD	8.32	5.97	4.44	3.13	2.91	2.75	2.59	2.11	1.94	1.31	1.03
MD	206	126	96	68	62	55	50	40	42	26	25
ICT (variable quantization)											
RMSE	15.47	9.60	7.34	4.83	4.46	4.29	4.22	2.70	2.25	1.46	1.26
PSNR	24.31	28.45	30.79	34.43	35.12	35.46	35.60	39.47	41.04	44.80	46.07
bpp	0.58	0.87	1.04	1.45	1.47	1.48	1.53	2.33	2.35	2.61	2.62
CR	13.75	9.24	7.72	5.51	5.45	5.42	5.24	3.43	3.41	3.07	3.05
NK	1.01	1.01	1.00	1.00	1.00	1.00	1.00	1.00	1.00	1.00	1.00
SC	0.98	0.99	0.99	1.00	1.00	1.00	1.00	1.00	1.00	1.00	1.00
NAE	0.04	0.03	0.02	0.01	0.01	0.01	0.01	0.01	0.01	0.00	0.00
LMSE	0.00	0.00	0.00	0.00	0.00	0.00	0.00	0.00	0.00	0.00	0.00
AD	8.50	6.03	4.60	3.00	2.72	2.64	2.62	1.75	1.52	1.01	0.87
MD	236	142	96	60	60	46	48	34	36	15	12

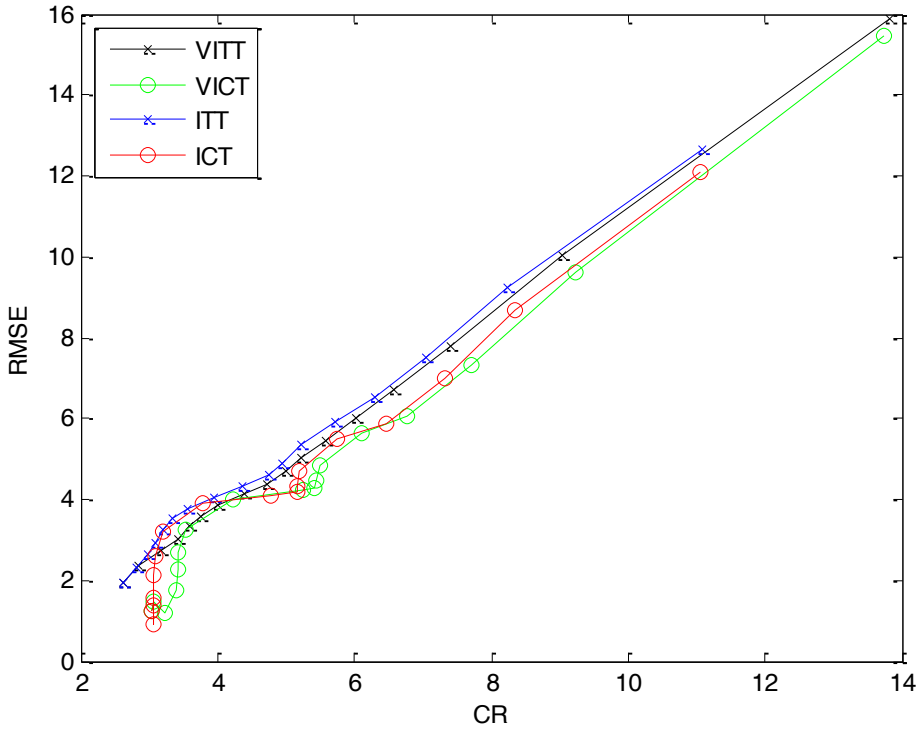

Figure 4.16: RMSE vs. CR plot for 8X8 compression of the scanned Hand-written letter

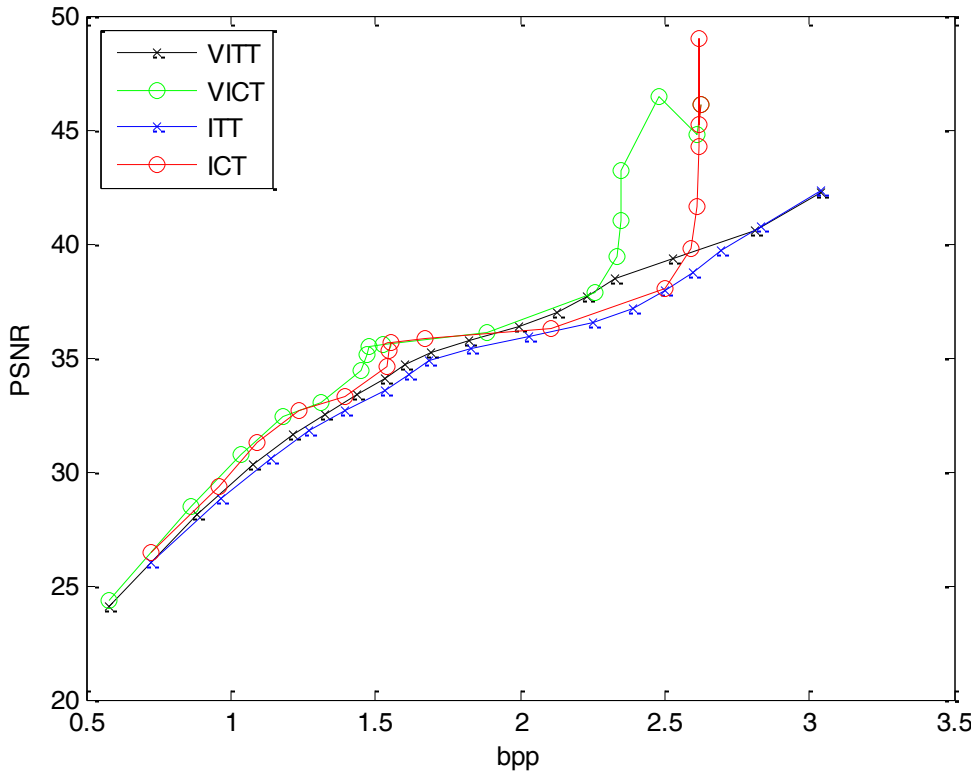

Figure 4.17: PSNR vs. bpp plot for 8X8 compression of the scanned Hand-written letter

By carrying an analysis similar to the one done previously, it can be deduced from the performance plots in Figs. 4.16 and 4.17 along with the data in Tables 4.6 and 4.7 that compression with variable quantization gives a slightly better performance than compression with standard quantization for both ITT and ICT.

From the above discussion of compression results, it can be concluded that the performance of variable quantization is either better than or at least the same as that with standard quantization in the cases discussed. For images with high spectral activity, performance of variable quantization with ITT and ICT was found to be almost the same as with normal quantization (Section 4.4.3). For images with low or moderate frequency content, variable quantization leads to higher PSNR or lower RMSE especially at higher compression ratios (Sections 4.4.1, 4.4.2, 4.4.4 and 4.4.5). Moreover, the increase in the computational complexity by comparing variable quantization to standard quantization is nominal, as it amounts to a couple of shift operations only as shown in Table 4.1. Thus, it is beneficial to choose variable quantization over conventional quantization for image compression using ITT or ICT.

4.5 Summary

In the beginning of the Chapter, the shortcomings of the usual quantization technique used in compression of images have been presented, followed by the necessity for a variable quantization technique and as to how it can improve compression performance. A novel variable quantization technique has been proposed along with an encoding technique to avoid any additional transmission overhead. It has been shown that adopting the variable quantization does not alter the existing compression technique much. The additional computational complexity has also been shown to be insignificant. Finally, the simulations carried out on a variety of images

show that variable quantization offers improved compression performance, especially at higher frequencies for images with low or moderate spectral activity.

Chapter 5

Conclusion

Image compression is one of the widely popular branches of digital signal processing. It has found application in varied fields like communications, defense, entertainment and health industry. In view of its wide spread utilization, there is a strong demand for efficient compression algorithms that are easy to implement and at the same time offer good quality reconstruction, even at high rates of compression.

The goal of this thesis is to compare the performance of compression based on ITT to that of the ICT- based compression and identify areas where ITT can be a viable alternative. This work also proposes a method to enhance the lossy compression algorithm by introducing a variable quantization technique thereby ensuring better image quality even at high compression rates.

It is undisputable that, conventionally discrete cosine transform has been the preferred choice for majority of the compression algorithms. Its popularity may be attributed to some of its features such as the ease of implementation and high energy compaction. However, it has been established time and over again that there cannot be a single transform that is best suited for compressing various types of image. Hence, it is justifiable to study the performance of ITT, implemented using a suitable image compression algorithm, compare it with that of ICT, and identify scenarios where ITT may be a favorable choice.

Usually, images have a heterogeneous distribution of detail over their area. So when the image is divided into blocks for compression, some of the blocks can have intricate detail and thus be sensitive to high amounts of quantization whereas the rest of the blocks would be robust to the

same. The quantization procedure carried during the compression scheme described in Section 3.2.1 treats all the image blocks similarly. As a result, the image blocks sensitive to quantization diminish the quality of the reconstructed image at high levels of compression. Reducing the overall quantization factor improves the quality but at the cost of the amount of compression achieved. In order to achieve better image quality even at high compression levels, it is apt to use higher quantization factor for blocks that can withstand excessive quantization and lower factor for blocks sensitive to quantization. Therefore, it is worth the effort to identify techniques to adapt the quantization used during compression, according to the characteristics of the image block without any additional computational or transmission overhead.

In this work, ITT of size 8×8 has been realized using a multiplier-free fast implementation using just add and shift operations. The arithmetic complexity of the fast ITT has been shown to be less than that of popular fast DCT and ICT implementations. The image compression performance of ITT and ICT have been evaluated and compared for diverse input images. The nature of images more suited for compression using ITT and using ICT have been identified based on SFM and SAM characteristics of the images. Through simulations it has been shown that the performance of ITT is about the same as that with ICT in most of the cases. Though the compression performance of ITT can be slightly inferior to ICT for images with high predictability (SAM), it provides a better performance than ICT does for images with low SAM, as illustrated for inter-coding images (Figs. 3.18 and 3.21). This could find a major application in the field of video compression where the concept of interceding is used.

The performances of ITT and ICT with and without variable quantization have also been compared in this thesis. When variable quantization is employed, the image blocks have been discriminated based on their sensitivity to quantization. The blocks that are robust to quantization

undergo double the quantization than the rest of the blocks. The additional computational complexity resulting from making the quantization variable has been shown to be negligible involving just a shift operation. The transmission overhead resulting from the requirement to transmit the variable quantization information has been avoided by the modified RLE that has been introduced. The image compression performances of ITT and ICT have been evaluated and compared for variable and fixed quantization cases using the PQE parameters and the performance curves. It has been found that the performance of variable quantization-based compression is either superior to or on par with that of the standardized compression technique for the images analyzed. Images with low or moderate frequency content were found to profit the most from variable quantization. This results in a better quality reconstructed image for a given compression ratio when variable quantization is employed. It can also be interpreted that higher compression ratios are possible for a fixed level of expected quality in the reconstructed image when variable quantization is used.

5.1 Future Work

While the strength of fast DCT designs lie in exploiting trigonometric properties, fast ITT designs can be developed by maneuvering its polynomial properties. Since polynomial theory is very well-developed, there is a possibility of developing more efficient ITT implementations.

The variable quantization technique proposed in this thesis can be further enhanced by differentiating the image blocks into more than two sets based on their sensitivity to quantization. The best compression could then be obtained by subjecting each set of blocks to a suitable level of quantization without sacrificing the image quality. Further research may be carried out to

customize the threshold value used to distinguish between the image blocks based on the type of image being compressed.

References

[1] Oppenheim, V. Alan Discrete-time signal processing 3rd ed Upper Saddle River : Pearson, c2010.

[2] Gonzalez, C. Rafael Digital image processing 3rd ed Upper Saddle River, N.J. ; Harlow : Pearson/Prentice Hall, c2008.

[3] Waggoner, Ben, Compression for great video and audio : master tips and common sense, 2nd ed Burlington, MA : Focal Press, c2010.

[4] R. Mukundan, S. H. Ong, and P. A. Lee, "Image analysis by Tchebichef moments," IEEE Trans. Image Process., vol. 10, no. 9, pp. 1357–1364,September 2001.

[5] K. Nakagaki and R. Mukundan, "A fast 4x4 forward discrete Tchebichef transform algorithm," IEEE Signal Process. Lett., 2007.

[6] Feig, Ephraim, Winograd, and Shmuel, "Fast algorithms for the discrete cosine transform," IEEE Trans. Signal Process., vol. 40, no. 9, pp. 2174– 2193, 1992.

[7] C. Loeffler, A. Ligtenberg, and G. S. Moschytz, "Practical fast 1-D DCT algorithms with 11 multiplications," IEEE International Conference on Acoustics, Speech, and Signal Processing, pp. 988–991 vol.2, May 1989.

[8] Y. Arai, T. Agui, and M. Nakajima, "A fast DCT-SQ scheme for images," Trans. IEICE, vol. E-71, no. 11, pp. 1095–1097, 1988.

[9] S. Ishwar, P. K. Meher, and M. N. S. Swamy, "Discrete Tchebichef transform-A fast 4x4 algorithm and its application in image/video compression," in IEEE International Symp. on Circuits and Systems, May 2008, pp. 260–263.

[10] S. Prattipati S. Iswar, M.N.S. Swamy and P.K. Meher, “A Fast 8X8 Integer Tchebichef Transform and Comparison with Integer Cosine Transform”, in IEEE International Midwest Conf. on Circuits and Systems, August 2013, pp. 1294 - 1297.

[11] Joint Collaborative Team on Video Coding (JCT-VC) of ITU-T SG16 WP3 and ISO/IEC JTC1/SC29/WG11 7th Meeting: Geneva, CH, 21-30 November, 2011.

[12] H. Rosengren, " Multivariable orthogonal polynomials and coupling coefficients for discrete series representations," *SIAM J. Math. Anal., vol. 30, no. 2, pp.233-272, 1999.*

[13] A.F. Nikiforov, S.K. Suslov and V.B. Uvarov, *Classical Orthogonal Polynomials of a Discrete Variable*. Springer Berlin 1991.

[14] Sujata Ishwar, “Discrete Tchebichef Transform and Its Application to Image/Video Compression”, M.A. Sc. Thesis, June 2008, Concordia University,Montreal.

[15] R. Mukundan, “Transform coding using discrete Tchebichef polynomials,” Proc. of IASTED International Conference on Visualization Imaging and Image Processing, pp. 270–275, August 2006.

[16] D.D. Fazio, S. Cavalli and V. Aquilanti, "Orthogonal polynomials of a discrete variable as expansion basis sets in quantum mechanics: Hyperquantization Algorithm," *International journal of Quantum Chemistry,* vol.93, pp.91-111, March 2003.

[17] W. Koepf, "Identities for families of orthogonal polynomials and special functions," *Integral Transforms and Special Functions, vol. 5, pp. 69-102, May 1997.*

[18] Richardson, E.G. Iain, *The H.264 advanced video compression standard. 2nd ed.* Hoboken, N.J. : Wiley, 2010.

[19] W.B. Pennebaker and J.L. Mitchell, *JPEG still image data compression standard.* Norwell MA, USA: Kluwer Academic Publishers, 1992.

[20] G. Szego, *Orthogonal polynomials. 4th ed.* American Mathematical Society Colloquium Publications. Vol. XXIII., 1975.

[21] A. Eskicioglu, "Quality measurement for monochrome compressed images in the past 25 years in Proc. of IEEE conference on Acoustics, Speech and Signal Processing, 2000 pp. 1907-1910.

[22] S. Grgic, M. Mrak, and M. Grgic, "Comparison of JPEG Image Coders," Proc. 3rd Int. Symp on Video Processing and Multimedia Communications,VIPromCom-2001, Zadar, Croatia, 2001, pp. 79-85.

[23] A. M. Eskicioglu and P. S. Fisher, "Image quality measures and their performance," IEEE Trans. Commun., vol. 43, no. 12, pp. 2959–2965, December 1995.

[24] Mathworks website. [Online].

Available: http://www.mathworks.com/

[25] Digital Image Processing Database [Online].

Available:http://www.imageprocessingplace.com/root_files_V3/image_databases.htm

[26] CVG-UGR image database. [Online].

Available: http: //decsai.ugr.es/cvg/dbimagenes/g256.php

[27] Footage: Small World Productions, Inc; Tourism New Zealand.

Producer: Gary F. Spradling | Music: Steve Ball

[28] Ramakrishna Kakarala and Ravikiran Bagadi, "A Method for Signalling Block-AdaptiveQuantization in Baseline Sequential JPEG," in IEEE TENCON, May 2009.

[29] S. Prattipati, M.N.S. Swamy and P.K. Meher, "A Variable Quantization technique for image compression using Integer Tchebichef Transform", presented at the IEEE International

Conference on Information, Communications and Signal Processing (ICICS), December 2013.

[30] Rabindranath Tagore articles. [Online].

Available: http://www.parabaas.com/rabindranath/articles/pMeyer.html